

1 **Estimating the atmospheric concentration of Criegee**
2 **intermediates and their possible interference in a FAGE-LIF**
3 **instrument**

4 Anna Novelli^{1,2}, Korbinian Hens¹, Cheryl Tatum Ernest^{1,3}, Monica Martinez¹, Anke C.
5 Nölscher^{1,4}, Vinayak Sinha⁵, Pauli Paasonen⁶, Tuukka Petäjä⁶, Mikko Sipilä⁶, Thomas Elste⁷,
6 Christian Plass-Dülmer⁷, Gavin J. Phillips^{1,8}, Dagmar Kubistin^{1,7,9}, Jonathan Williams¹, Luc
7 Vereecken^{1,2}, Jos Lelieveld¹ and Hartwig Harder¹

8

9 [1] {Atmospheric Chemistry Department, Max Planck Institute for Chemistry, 55128 Mainz,
10 Germany}

11 [2] Now at: {Institute of Energy and Climate Research, IEK-8: Troposphere,
12 Forschungszentrum Jülich GmbH, 52428 Jülich, Germany}

13 [3] Now at: {Department of Neurology University Medical Center of the Johannes Gutenberg
14 University Mainz, 55131 Mainz}

15 [4] Now at: {Division of Geological and Planetary Sciences, California Institute of
16 Technology, Pasadena, USA}

17 [5] {Department of Earth and Environmental Sciences, Indian Institute of Science Education
18 and Research Mohali, Sector 81 S.A.S. Nagar, Manauli PO, Mohali 140 306, Punjab, India}

19 [6] {Department of Physics., P.O. Box 64. 00014 University of Helsinki, Finland}

20 [7] {German Meteorological Service, Meteorological Observatory Hohenpeissenberg
21 (MOHp), 83282 Hohenpeissenberg, Germany}

22 [8]{Department of Natural Sciences, University of Chester, Thornton Science Park, Chester,
23 CH2 4NU, UK}

24 [9] {University of Wollongong, School of Chemistry, Wollongong, Australia}

25

1 Correspondence to: H. Harder (hartwig.harder@mpic.de)

2 **Abstract**

3 We analysed the extensive dataset from the HUMPPA-COPEC 2010 and the HOPE 2012
4 field campaigns in the boreal forest and rural environments of Finland and Germany,
5 respectively, and estimated the abundance of stabilised Criegee intermediates (SCI) in the
6 lower troposphere. Based on laboratory tests, we propose that the background OH signal
7 observed in our IPI-LIF-FAGE instrument during the afore-mentioned campaigns is caused at
8 least partially by SCI. This hypothesis is based on observed correlations with temperature and
9 with concentrations of unsaturated volatile organic compounds and ozone. Just like SCI, the
10 background OH concentration can be removed through the addition of sulfur dioxide. SCI
11 also adds to the previously underestimated production rate of sulfuric acid. An average
12 estimate of the SCI concentration of $\sim 5 \times 10^4$ molecules cm^{-3} (with an order of magnitude
13 uncertainty) is calculated for the two environments. This implies a very low ambient
14 concentration of SCI, though, over the boreal forest, significant for the conversion of SO_2
15 into H_2SO_4 . The large uncertainties in these calculations, owing to the many unknowns in the
16 chemistry of Criegee intermediates, emphasise the need to better understand these processes
17 and their potential effect on the self-cleaning capacity of the atmosphere.

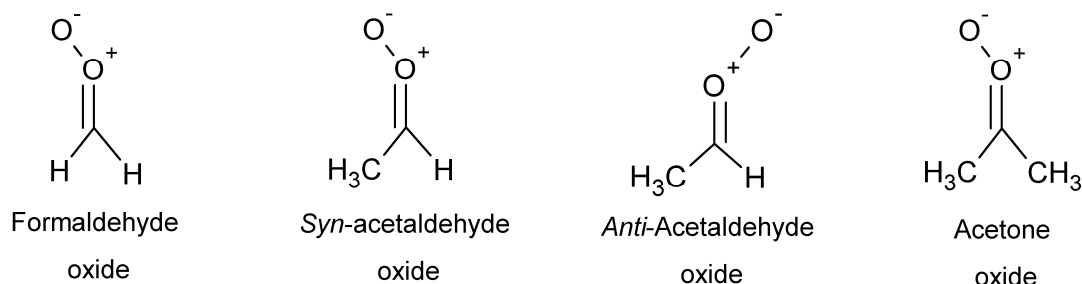
18

19 **1 Introduction**

20 Criegee intermediates (CI), or carbonyl oxides, are formed during the ozonolysis of
21 unsaturated organic compounds (Criegee, 1975; Johnson and Marston, 2008; Donahue et al.,
22 2011): in the gas phase ozone attaches to a double bond forming a primary ozonide (POZ)
23 that quickly decomposes forming a Criegee intermediate and a carbonyl compound. The CI

1 can exist as thermally stabilised CI (SCI) or as chemically activated CI (Kroll et al.,
 2 2001;Drozd et al., 2011), where the chemically activated CI have high energy content and in
 3 the atmosphere either undergo unimolecular decomposition, or are stabilised by collisional
 4 energy loss forming SCI.

5 For many decades the chemistry of Criegee intermediates was investigated both with
 6 theoretical and indirect experimental studies as reviewed in detail by Johnson and Marston
 7 (2008), Vereecken and Francisco (2012), and Vereecken et al. (2015). During the last few
 8 years, numerous experimental studies specifically on stabilised Criegee intermediates have
 9 been performed following their first detection by Welz et al. (2012). Many laboratories have
 10 now detected SCI with various techniques (Berndt et al., 2012;Mauldin III et al.,
 11 2012;Ouyang et al., 2013;Taatjes et al., 2013;Ahrens et al., 2014;Buras et al., 2014;Liu et al.,
 12 2014a;Sheps et al., 2014;Novelli et al., 2014b;Stone et al., 2014;Chhantyal-Pun et al.,
 13 2015;Lee, 2015;Newland et al., 2015a;Fang et al., 2016a;Smith et al., 2016) and have
 14 confirmed that they are very reactive towards many atmospheric trace gases. Currently, the
 15 most studied Criegee intermediates are formaldehyde oxide, CH_2OO , acetaldehyde oxide,
 16 CH_3CHOO (*syn* and *anti*, i.e. with the outer oxygen pointing towards or away from an alkyl
 17 group, respectively) and acetone oxide, $(\text{CH}_3)_2\text{COO}$.



18

19 The importance of stabilised Criegee intermediates as oxidants in the atmosphere depends on
 20 the rate coefficient of their reaction with water vapour as the latter is ubiquitously present in

1 relatively high concentrations in the boundary layer (between 10^{16} to 10^{17} molecules cm^{-3}).
2 The rate of this reaction strongly depends on the CI conformation (Aplincourt and Ruiz-
3 López, 2000; Tobias and Ziemann, 2001; Ryzhkov and Ariya, 2003; Kuwata et al.,
4 2010; Anglada et al., 2011; Anglada and Sole, 2016; Chen et al., 2016; Lin et al., 2016; Long et
5 al., 2016) and until now the rate coefficient has been measured for *anti*-CH₃CHOO (Taatjes
6 et al., 2013; Sheps et al., 2014) while lower limits have been determined for CH₂OO (Stone et
7 al., 2014), *syn*-CH₃CHOO (Taatjes et al., 2013; Sheps et al., 2014) and (CH₃)₂COO (Huang et
8 al., 2015; Newland et al., 2015b). The uncertainties in these rate coefficients make it difficult
9 to estimate the importance of Criegee intermediates and the impact they may have as oxidants
10 in the atmosphere. Additionally, recent studies (Berndt et al., 2014b; Chao et al., 2015; Lewis
11 et al., 2015; Smith et al., 2015; Lin et al., 2016) showed that the reaction between CH₂OO and
12 water dimers (present in the ppmv range in the atmosphere (Shillings et al., 2011)) is faster
13 than the reaction with water vapor, in agreement with the several theoretical studies
14 (Ryzhkov and Ariya, 2004; Chen et al., 2016; Lin et al., 2016) which indicate the reaction with
15 water dimers to be between 400 and 35,000 times faster than the reaction with water vapor
16 depending on the conformers. Another important reaction of SCI that depends on the SCI
17 conformation is their unimolecular decomposition. The decomposition rate and product
18 formed depend on the SCI conformer structure. *Anti*-SCI are likely to isomerise via the ester
19 channel forming an ester or an acid as final product while *syn*-SCI will form a vinyl
20 hydroperoxide (VHP) which promptly decomposes forming hydroxyl radicals (OH) and a
21 vinoxy radical (Paulson et al., 1999; Johnson and Marston, 2008; Drozd and Donahue,
22 2011; Vereecken and Francisco, 2012; Kidwell et al., 2016). Larger and more complex
23 conformers such as hetero-substituted or cyclic structures are subject to additional
24 unimolecular rearrangements (Vereecken and Francisco, 2012). On the unimolecular

1 decomposition rates and products few experimental data are available (Horie et al.,
2 1997;Horie et al., 1999;Fenske et al., 2000a;Novelli et al., 2014b;Kidwell et al., 2016;Fang et
3 al., 2016a;Smith et al., 2016), but more is available from theoretical studies explicitly
4 focusing on the path followed by different conformers (Anglada et al., 1996;Aplincourt and
5 Ruiz-López, 2000;Kroll et al., 2001;Zhang and Zhang, 2002;Nguyen et al., 2009b;Kuwata et
6 al., 2010).

7 Most of the experimental and theoretical information described above refers to the smaller
8 conformers. These compounds are likely to be formed relatively efficiently in the atmosphere
9 as they can originate from any unsaturated compound with a terminal double bond, but they
10 do not represent the entire Criegee intermediate population.

11 As SCI were found to react quickly with many trace gases, various model studies were
12 performed on the impact SCI have as oxidants in the atmosphere (Vereecken et al., 2012;Boy
13 et al., 2013;Percival et al., 2013;Pierce et al., 2013;Sarwar et al., 2013;Sarwar et al.,
14 2014;Novelli et al., 2014b;Vereecken et al., 2014). Some of these studies focused in
15 particular on the possible impact that SCI might have on the formation of sulfuric acid
16 (H_2SO_4) in the gas phase, following Mauldin III et al. (2012) who suggested that Criegee
17 intermediates are the missing SO_2 oxidant needed to close the sulfuric acid budget over a
18 boreal forest. This is supported by theoretical and laboratory studies that have determined a
19 rate coefficient between SCI and sulfur dioxide (SO_2) of the order of $10^{-11} \text{ cm}^3 \text{ molecule}^{-1} \text{ s}^{-1}$
20 (Aplincourt and Ruiz-López, 2000;Jiang et al., 2010;Kurtén et al., 2011;Vereecken et al.,
21 2012;Welz et al., 2012;Taatjes et al., 2013;Liu et al., 2014b;Sheps et al., 2014;Stone et al.,
22 2014). As the main atmospherically relevant oxidiser of SO_2 in the gas phase is the OH
23 radical with a rather slow rate coefficient at ambient temperature and pressure of 2×10^{-12}
24 $\text{cm}^3 \text{ molecule}^{-1} \text{ s}^{-1}$ (Atkinson et al., 2004), the high rate coefficient for SO_2 oxidation would

1 allow SCI to have a significant impact on the H_2SO_4 formation even if present in small
2 concentrations. The model studies have shown that, depending on the environment, SCI can
3 have a potentially important impact on H_2SO_4 formation. All these studies are affected by
4 large uncertainties and many simplifications used for coping with the paucity of data on the
5 reactions of specific SCI with various trace gas species, on the speciation of SCI, and on the
6 steady state concentration of SCI in the troposphere. Until now no direct or reproducible
7 indirect method was able to determine the steady state concentration of SCI in the lower
8 troposphere.

9 In this paper, we firstly estimate the concentration of SCI in the lower troposphere, based on
10 the data collected during the HUMPPA-COPEC 2010 campaign (Williams et al., 2011) in a
11 Boreal forest in Finland and the HOPE 2012 campaign in rural southern Germany. The
12 budget of SCI is analyzed using four different approaches: 1) based on an unexplained H_2SO_4
13 production rate (Mauldin III et al., 2012); 2) from the measured concentrations of unsaturated
14 volatile organic compounds (VOC); 3) from the observed OH reactivity (Nölscher et al.,
15 2012); and 4) from an unexplained production rate of OH (Hens et al., 2014). Secondly, we
16 present measurements obtained using our inlet pre-injector laser-induced fluorescence assay
17 by gas expansion technique (IPI-LIF-FAGE) (Novelli et al., 2014a) during the HUMPPA-
18 COPEC 2010 and the HOPE 2012 campaigns. A recent laboratory study performed with the
19 same instrumental setup showed that the IPI-LIF-FAGE system is sensitive to the detection
20 of the OH formed from unimolecular decomposition of SCI (Novelli et al., 2014b). Building
21 on this study, the background OH (OH_{bg}) (Novelli et al., 2014a) measured during the two
22 field campaigns is investigated in comparison with many other trace gases in order to assess
23 if the observations in controlled conditions are transferable to the ambient conditions.

24

2 Instrumentation and field sites

2.1 IPI-LIF-FAGE description

A comprehensive description of the IPI-LIF-FAGE ground-based instrument, HORUS (Hydroxyl Radical Measurement Unit based on fluorescence Spectroscopy), is given by Novelli et al. (2014a) and only some important features of the instrument are highlighted here. The IPI-LIF-FAGE instrument consists of: the inlet pre-injector (IPI), the inlet and detection system, the laser system, the vacuum system and the instrument control and data acquisition unit. The air is drawn through a critical orifice into a low pressure region (~ 300 - 500 Pa) where OH molecules are selectively excited by pulsed UV light around 308 nm. The light is generated at a pulse repetition frequency of 3 kHz by a Nd:YAG pumped, pulsed, tunable dye laser system and is directed into a multipass "White cell" making 32 passes through the detection volume (White, 1942). The air sample intersects the laser beam and the fluorescence signal from the excited OH molecules is detected using a gated micro-channel plate (MCP) detector. IPI, situated in front of the instrument inlet, is used to measure a chemical zero to correct for possible internal OH signal generation. An OH scavenger (propene) is added to the sample air 5 cm in front of the inlet pinhole in a concentration that allows a known, high proportion of atmospheric OH to be scavenged (~ 90 %). The OH scavenger is added every two minutes so that the instrument measures a total OH signal (OH_{tot}) when the OH scavenger is not injected and a background OH signal (OH_{bg}) when the OH scavenger is injected. The difference between these two signals yields the atmospheric OH concentration (OH_{atm}). The efficiency of this technique for measuring OH with this particular LIF-FAGE instrument is described together with the IPI characterisation in Novelli et al. (2014a). The OH calibration of the HORUS instrument is obtained via the production of

1 a known amount of OH and hydroperoxyl radicals (HO_2) from the photolysis of water at 185
2 nm using a mercury lamp. A more detailed description of the instrument calibration is
3 reported by Martinez et al. (2010) and Hens et al. (2014). A calibration factor for the
4 background OH signal observed by the HORUS instrument is currently not available.
5 Therefore, this signal will be discussed and plotted in OH fluorescence counts per seconds
6 (cps) measured by the MCP, normalized by the laser power and corrected for quenching and
7 sensitivity changes towards the detection of OH. The sensitivity of the instrument towards the
8 OH radical is affected by: alignment of the white cell, optical transmission of the
9 components, sensitivity of the MCP, water vapor, internal pressure, and internal temperature
10 (Martinez et al., 2010). These factors affect the sensitivity of HORUS towards the
11 background OH in a similar manner as they mainly impact the sensitivity of the instrument to
12 the detection of OH.

13 We hypothesise that the OH_{bg} is formed chemically within the IPI-LIF-FAGE instrument.
14 Laser induced production of OH radicals was thoroughly tested in the laboratory and in the
15 field (Novelli et al., 2014a) showing that this background OH signal is not induced by the
16 laser beam from double pulsing, nor from air stagnating in the detection cell. By changing the
17 laser power, no quadratic dependency of the OH_{bg} was observed even at night time, when the
18 contribution of the OH_{bg} to the OH_{tot} measured by the instrument is highest (Novelli et al.,
19 2014a). In addition, during the HUMPPA-COPEC 2010 and HOPE 2012 campaigns, the
20 correlation coefficient of the OH_{bg} with the laser power was $R = 0.002$ and $R = 0.2$,
21 respectively.

22 In contrast, ozonolysis of alkenes performed during laboratory tests showed that the IPI-LIF-
23 FAGE instrument is sensitive to the OH formed from unimolecular decomposition of SCI
24 within the low pressure section of the instrument (Novelli et al., 2014b).

1 Recently, most of the LIF-FAGE instruments have been augmented with the titration of
2 OH_{atm} in different environments to determine their background (Amédro, 2012;Mao et al.,
3 2012;Griffith et al., 2013;Woodward-Massey et al., 2015;Griffith et al., 2016;Tan et al.,
4 2016). Some of these instruments showed the presence of an unknown interference (Mao et
5 al., 2012;Griffith et al., 2013;Tan et al., 2016) while for others no clear conclusions were
6 drawn (Amédro, 2012;Woodward-Massey et al., 2015). In addition, laboratory studies (Fuchs
7 et al., 2016;Griffith et al., 2016) have shown similarity with what was observed with the IPI-
8 LIF-FAGE during experiments of ozonolysis of alkenes although the origin of the OH signal
9 was not uniquely attributed to a particular mechanism.

10 Our hypothesis is that the OH_{bg} measured in ambient air with the IPI-LIF-FAGE at least
11 partially originates from unimolecular decomposition of SCI. Section 4 describes the
12 observed behaviour of the signal during the campaigns and its relationship to other observed
13 chemical tracers and discusses if this is compatible with our hypothesis.

15 **2.2 Measurement site and ancillary instrumentation**

16 We present measurements from two sites, a boreal forest site in Finland and a rural site in
17 Southern Germany. The HUMPPA-COPEC 2010 (Hyytiälä United Measurements of
18 Photochemistry and Particles in Air – Comprehensive Organic Precursor Emission and
19 Concentration study) campaign took place during summer 2010 at the SMEAR II station in
20 Hyytiälä, Finland (61° 51' N, 24°17' E, 181 m a.s.l.) in a boreal forest dominated by Scots
21 Pines (*Pinus Silvestris L.*). The site hosts continuous measurements of several trace gases and
22 meteorological parameters as well as aerosol particles concentrations, size distributions and
23 composition (Junninen et al., 2009). Further details and a more complete description of the

1 site, the instrumentation and the meteorological conditions during the campaign can be found
2 in Williams et al. (2011) and Hens et al. (2014). A brief description of the instruments used in
3 this study is given here. Ozone was measured by a UV photometric gas analyser (Model 49,
4 Thermo Electron Corporation). A gas chromatograph (GC, Agilent Technologies 6890A)
5 coupled to a mass-selective detector (MS, Agilent Technologies MSD 5973 *inert*) was used
6 for the measurements of biogenic volatile organic compounds (BVOC) (Yassaa et al., 2012).
7 The total OH reactivity was measured by the comparative reactivity method (CRM) (Sinha et
8 al., 2008) for two different heights, one within and one above the canopy (18 and 24 m,
9 respectively) (Nölscher et al., 2012). CRM uses an in-situ kinetics experiment to measure the
10 OH reactivity based on the competitive scavenging of OH by a reference gas (pyrrole) and
11 atmospheric OH reactants. The overall uncertainty of the method during deployment was
12 16% with a limit of detection of 3 s^{-1} (Hens et al., 2014). Sulfur dioxide (SO_2) concentration
13 was measured with a fluorescence analyzer (Model 43S, Thermo 20 Environmental
14 Instruments Inc.). Aerosol number size distributions between 3 nm and 950 nm were
15 measured with a Differential Mobility Particle Sizer (DMPS) (Aalto et al., 2001). The size
16 distributions were used for calculating the loss rate of gas-phase sulfuric acid via
17 condensation sink (CS) with the method presented by Kulmala et al. (2001). Sulfuric acid
18 (H_2SO_4) and OH radical concentrations were measured on the ground with a chemical
19 ionization mass spectrometer (CIMS; (Petäjä et al., 2009)). Time series of the measured trace
20 gases are available in the study from Nölscher et al. (2012) and Hens et al. (2014). The
21 average concentrations and their 1σ variability are listed in Table 1 and Table SI-2. For the
22 first period of the campaign, between the 27th and the 31st of July, the IPI-LIF-FAGE
23 instrument was run on the ground side-by-side with the CIMS. On the 2nd of August the IPI-
24 LIF-FAGE instrument was moved to the top of the HUMPPA tower above the canopy and

1 measured there for the remainder of the campaign (12th of August). The data are therefore
2 separated into ground and tower periods

3 The HOPE 2012 (Hohenpeißenberg Photochemistry Experiment) campaign was conducted
4 during the summer of 2012 at the Meteorological Observatory in Hohenpeißenberg, Bavaria,
5 Germany (47° 48' N, 11° 2' E). The observatory is a Global Atmosphere Watch (GAW)
6 station operated by the German Meteorological Service (DWD) and is located at an altitude
7 of 985 m a.s.l. and about 300 m above the surrounding terrain, mainly consisting of meadows
8 and coniferous forests. More information about the site can be found in Handisides et al.
9 (2003). Ozone was measured by UV absorption with TEI 49C (Thermo Electron Corporation,
10 Environmental Instruments) (Gilge et al., 2010). Non-methane hydrocarbons (NMHC) were
11 measured with a GC-flame ionization detection (FID) system (series 3600CX, Varian,
12 Walnut Creek, CA, USA) (Plass-Dülmer et al., 2002). BVOC were detected using a GC
13 (Agilent 6890) with a FID running in parallel with a MS (Agilent Technologies MSD 5975
14 *inertXL*) described by Hoerger et al. (2014). Photolysis frequencies ($J(\text{NO}_2)$ and $J(\text{O}^1\text{D})$) were
15 measured next to the IPI-LIF-FAGE with a set of filter radiometers (Handisides et al., 2003).
16 The OH reactivity was measured with two instruments for a short period of time from the 10th
17 until the 18th of July. One method was the CRM and the same instrument was used as during
18 the HUMPPA-COPEC 2010 campaign. The second method was a new application of the
19 DWD CIMS instrument (Berresheim et al., 2000) which also measured H_2SO_4 and OH
20 radicals. As the data will be used only in a qualitative way for the current study, a very short
21 description of this novel technique is given here and details will be presented in a future
22 publication. With the CIMS instrument, OH radicals are measured by converting them into
23 H_2SO_4 after reaction with SO_2 in a chemical reactor and subtraction of a corresponding
24 background after scavenging the OH with propane (Berresheim et al, 2000). A second SO_2

1 titration zone was used 15 cm (or 140 ms) downstream of the first injection to determine the
 2 OH decay from OH radicals generated in the UV-calibration zone immediately upstream of
 3 the first titration. The difference between these two titration zones in two consecutive 2.5 min
 4 intervals allows the determination of the OH decay, after correcting for ambient OH and wall
 5 losses. The uncertainty is estimated at $\pm 2 \text{ s}^{-1}$ and the limit of detection is 2 s^{-1} . SO_2
 6 concentration was measured with a fluorescence analyzer and aerosol size distributions were
 7 measured and used to calculate the loss rate of gas-phase sulfuric acid due to CS formed by
 8 existing aerosol surface via the method presented by (Birmili et al., 2003). Time series of the
 9 measured trace gases are available in Figure SI-1. The average concentrations and their 1σ
 10 variability are listed in Table 1 and Table SI-2

11

12 **3 SCI concentrations during HUMPPA-COPEC 2010 and HOPE 2012**

13 **3.1 Missing H_2SO_4 oxidant**

14 The study by Mauldin III et al. (2012) in a boreal forest during the HUMPPA-COPEC 2010
 15 campaign showed a consistent discrepancy between the measured H_2SO_4 and the calculated
 16 gas phase H_2SO_4 concentration when considering oxidation of SO_2 from OH radical and the
 17 condensation onto pre-existing aerosol particles (CS, condensation sink) as the sole
 18 production and loss processes, respectively (Eq. 1).

$$19 \quad [\text{H}_2\text{SO}_4] = \frac{k_{\text{OH}+\text{SO}_2} \times [\text{OH}] \times [\text{SO}_2]}{\text{CS}} \quad (1)$$

20 The H_2SO_4 concentration is assumed to be in near-steady state: the lifetime of H_2SO_4 in the
 21 gas phase is of the order of minutes, i.e. spanning a similar time period compared to the
 22 variability in the production and loss pathways, ensuring fast response of the H_2SO_4

1 concentration to varying conditions. Minor deviations from steady state are not critical for the
 2 analysis performed in this study, given the uncertainties induced by other parameters.

3 On average the sulfuric acid in the gas phase calculated using Eq. 1 was only half of the total
 4 H₂SO₄ observed in the field and lied outside the uncertainties associated with the calculation
 5 of the formation channel and the condensation sink (Mauldin III et al., 2012). Although no
 6 unambiguous evidence links SCI to the missing oxidant, laboratory tests performed with a
 7 similar instrument (Berndt et al., 2012; Berndt et al., 2014a; Sipilä et al., 2014) confirmed the
 8 role that SCI could have in the oxidation of SO₂ and formation of H₂SO₄. Assuming that SCI
 9 are the only other species in addition to OH that oxidize SO₂ in the gas phase and knowing
 10 the rate coefficient of SCI and OH with SO₂, it is possible to calculate the steady state
 11 concentration of SCI in that environment:

$$12 \quad [H_2SO_4] = \frac{(k_{OH+SO_2} \times [OH] + k_{SCI+SO_2} \times [SCI]) \times [SO_2]}{CS} \quad (2)$$

13 The rate coefficient between OH and SO₂ at standard pressure is (2.04 ± 0.10) ×
 14 10⁻¹² (T/300)^{-0.27} cm³ molecule⁻¹ s⁻¹ (Atkinson et al., 2004). The rate coefficient of SCI with
 15 SO₂ was determined by several groups at (3.3 ± 2) × 10⁻¹¹ cm³ molecule⁻¹ s⁻¹, (Welz et al.,
 16 2012; Taatjes et al., 2013; Liu et al., 2014b; Sheps et al., 2014; Stone et al., 2014; Chhantyal-Pun
 17 et al., 2015; Newland et al., 2015a; Newland et al., 2015b; Foreman et al., 2016; Zhu et al.,
 18 2016). An earlier, lower value of ~ 5 × 10⁻¹³ cm³ molecule⁻¹ s⁻¹ (Mauldin III et al. (2012);
 19 Berndt et al. (2012)) appears to be hard to reconcile with the remaining literature, as
 20 extensively discussed in the supporting information.

21 Equation 2 allows for the calculation of a time series of SCI (Fig. SI-2) yielding an average
 22 [SCI] = (2.3 ± 2) × 10⁴ molecules cm⁻³.

1 A similar estimate of the SCI time series was derived for the HOPE 2012 campaign (Fig. SI-
 2 3). The H_2SO_4 concentration during this campaign can be mainly explained by the reaction
 3 between OH and SO_2 . Figure 1 shows the correlation between the total production rate of
 4 H_2SO_4 ($\text{P}(\text{H}_2\text{SO}_4)_{\text{tot}}$) calculated from the product of measured H_2SO_4 and the condensation
 5 sink, as well as the production rate of H_2SO_4 from the reaction of OH and SO_2 . The linear
 6 regression following the method of York et al. (2004) yields a slope of 0.90 ± 0.02 with a
 7 negligible intercept ($57 \pm 7 \text{ molecules cm}^{-3} \text{ s}^{-1}$). It should be noted that the H_2SO_4 budget for
 8 the HOPE 2012 campaign is nearly closed, such that the moderate fluctuations on the source
 9 data (CS, [OH], etc.) lead to very large relative uncertainties of the small missing H_2SO_4
 10 production term, and concomitantly the time series for the SCI concentration (Fig. SI-3)
 11 shows extreme variability reflecting this noise on the source data. On average, the [SCI]
 12 obtained is low, $(2 \pm 3) \times 10^4 \text{ molecules cm}^{-3}$, with no values in the time series exceeding 10^5
 13 molecule cm^{-3} .
 14 Repeating the above analysis using the low $k_{\text{SCI}+\text{SO}_2}$ value of Mauldin III et al. and Berndt et
 15 al. yields concentrations of $(1.6 \pm 2) \times 10^6$ and $(1 \pm 3) \times 10^6 \text{ molecule cm}^{-3}$ for the
 16 HUMPPA-COPEC and HOPE campaigns, respectively. It is interesting to notice that both
 17 values estimated with the fast and low $k_{\text{SCI}+\text{SO}_2}$ rate coefficient are in agreement with the
 18 concentrations calculated from measured VOC and O_3 for polluted and pristine environments,
 19 $1.9 \times 10^6 \text{ molecules cm}^{-3}$ and $4.5 \times 10^4 \text{ molecules cm}^{-3}$ respectively, from a previous study
 20 (Welz et al., 2012).

21

3.2 Measured unsaturated VOC

Another method to estimate the SCI concentration is based on their production and loss processes. In a forest SCI are expected to be formed from the ozonolysis of unsaturated BVOC. It is possible to calculate an average steady state concentration for SCI using the following equation

$$[SCI] = \sum_i \left(\frac{k_{VOC_i+O_3} \times [VOC_i] \times Y_{SCI}}{L_{SCI_{syn}}} \right) \times [O_3] \quad (3)$$

Where $k_{VOC_i+O_3}$ is the rate coefficient between the VOC_i and ozone (Table SI-2), Y_{SCI} is the yield of SCI in the ozonolysis reaction, and $L_{SCI_{syn}}$ is the total loss of *syn*-SCI. We assume $[SCI] \approx [SCI_{syn}]$ following the model described by Novelli et al. (2014b), which accounts for many possible losses of SCI including the reaction with water dimers and unimolecular decomposition. The latter study suggests that *anti*-acetaldehyde oxide and formaldehyde oxide react quickly with water and water dimers and that their contributions can be neglected. A yield of SCI formation (Y_{SCI}) of 0.4 was estimated based on the data by Hasson et al. (2001). The steady state concentration of SCI for the HUMPPA-COPEC 2010 campaign was calculated using the measured data for $[O_3]$ and $[VOC_i]$ and an average value of 40 s^{-1} (Novelli et al., 2014b) for $L_{SCI_{syn}}$ as this value was found to be rather constant and mainly dependent on the unimolecular decomposition rate of the SCI. Equation 3 allows for the calculation of a time series of SCI (Fig. SI-4) yielding an average $[SCI]$ of $\sim (5 \pm 4) \times 10^3$ molecules cm^{-3} .

During the HOPE 2012 campaign a larger number of unsaturated organic trace gases, both anthropogenic and biogenic, were measured (Table SI-1). For Y_{SCI} the same value of 0.4 was used while for $L_{SCI_{syn}}$ the value of 32 s^{-1} , obtained from the model described by Novelli et al.

(2014b) for the rural European environment, was used. Using these values in Eq. 3 results in $[SCI] = (7 \pm 6) \times 10^3 \text{ molecules cm}^{-3}$, obtained as an average of the SCI time series (Fig. SI-5). It should be noted that recent work on the unimolecular decomposition (Fang et al., 2016b; Long et al., 2016; Smith et al., 2016) yields loss rates significantly faster than used here; this implies that the $[SCI]$ obtained here could be an overestimate.

3.3 OH reactivity

During HUMPPA-COPEC 2010, between 27th July and 12th August, an average OH reactivity, $R = 9.0 \pm 7.6 \text{ s}^{-1}$, was measured. On average, the majority of the measured OH reactivity ($R_{unex} = 7.4 \pm 7.4 \text{ s}^{-1}$), 80 %, was not accounted for by the measured organic and inorganic trace gases (Fig. SI-6). Biogenic emissions comprised up to ~ 10 % of the total measured OH reactivity and up to half of the calculated OH reactivity (Fig. SI-6). As the measurement site was located in a pristine forest environment, affected only little by anthropogenic emissions (Williams et al., 2011), it is likely that a large fraction of the unexplained OH reactivity was formed by unmeasured primary emissions by the vegetation and secondary products of oxidation. By assuming that the unmeasured VOC are unsaturated, and by using a lumped rate coefficient, k_{VOC+OH} , between OH and the fraction of unspciated VOC of $7 \times 10^{-11} \text{ cm}^3 \text{ molecule}^{-1} \text{ s}^{-1}$, typical for an OH addition to a carbon-carbon double bond (Atkinson et al., 2004; Peeters et al., 2007), it is possible to estimate the concentration $[VOC_{unknown}]$ of VOC that would be necessary to close the OH reactivity budget (Eq. 4).

$$R_{unex} = k_{VOC+OH} \times [VOC_{unknown}] \quad (4)$$

Using Eq. 4, a time series for $[VOC_{unknown}]$ with an average of $(1 \pm 1) \times 10^{11} \text{ molecules cm}^{-3}$ is obtained. This value is substituted into Eq. 3 and a lumped rate for reaction of $[VOC_{unknown}]$

1 and O_3 of 7×10^{-17} molecules cm^{-3} is used. This value is based on the rate coefficient of the
2 measured VOC with O_3 weighted with their abundance (Table SI-1). The same Y_{SCI} and
3 $L_{SCI_{syn}}$, of 0.4 and $40 s^{-1}$, respectively, were used as described in section 3.2. With these
4 values, a time series of SCI (Fig. SI-7) with an average of $\sim (1 \pm 1) \times 10^5$ molecules cm^{-3} is
5 obtained. To this SCI concentration estimate, we add the SCI formed from the measured
6 unsaturated VOC, $[SCI] = (5 \pm 4) \times 10^3$ molecules cm^{-3} , to obtain the total SCI across all
7 VOC. As this estimate requires assumptions for the rate coefficient between $[VOC_{unknown}]$
8 and OH and O_3 , a sensitivity study probing the upper and lower bounds of this estimate is
9 described in the supplementary information.

10 During the HOPE 2012 campaign the total OH reactivity was on average $3.5 \pm 3.0 s^{-1}$. Using
11 the measured trace gas concentrations it is possible to calculate the expected OH reactivity
12 (Fig. SI-8). Table SI-2 lists all the species included in the calculation of the OH reactivity
13 with their rate coefficient with OH. An average value of $2.7 \pm 0.7 s^{-1}$ was calculated. Figure
14 SI-8 shows that half of the measured OH reactivity can be explained by methane, carbonyl
15 compounds (mainly acetaldehyde and propanal) and inorganic compounds which were
16 present in higher concentrations compared to the HUMPPA-COPEC 2010 campaign (Table
17 SI-2). On average, 24 % of the measured OH reactivity remains unexplained by the measured
18 trace gases. In contrast to the HUMPPA-COPEC 2010 campaign, in HOPE 2012 a more
19 complete speciation of VOC was measured (Table SI-1) and the site was influenced by
20 relatively fresh anthropogenic emissions. With the extensive VOC speciation available, the
21 reactivity budget can virtually be closed, but any remaining unexplained OH reactivity could
22 still be due to unmeasured VOC. The time series for this unexplained OH reactivity, typically
23 about $\sim 1 s^{-1}$, shows very large variability as it reflects the statistical noise of the small
24 difference between measured and calculated OH reactivities, both of which are associated

1 with variability. The resulting [SCI] time series (Fig. SI-9) is also highly variable, and yields
2 a low average SCI concentration of $(2.0 \pm 1.5) \times 10^4$ molecules cm^{-3} , with no values
3 exceeding 6×10^4 molecule cm^{-3} .

4 The total SCI is then obtained by summing the SCI predicted from the measured VOC and
5 from the unexplained OH reactivity, leading to a total SCI concentration of $(7 \pm 6) \times 10^3$
6 molecules cm^{-3} .

8 **3.4 Unexplained OH production rate**

9 During the HUMPPA-COPEC 2010 campaign, the comprehensive measurements (Williams
10 et al., 2011) allowed the calculation of a detailed OH budget (Hens et al., 2014). Most of the
11 OH production during daytime is due to photolysis of O_3 and recycling of HO_2 back to OH
12 via reactions with NO and O_3 . This result holds for both high ($R > 15 \text{ s}^{-1}$) and low ($R \leq 15 \text{ s}^{-1}$)
13 OH reactivity episodes during the campaign. While the OH budget can be closed during
14 daytime ($J(\text{O}^1\text{D}) > 3 \times 10^{-6} \text{ s}^{-1}$) for low OH reactivity periods, during periods with high OH
15 reactivity there was a large unexplained production rate of OH, $P_{\text{OH}}^{\text{unexplained}} = (2 \pm 0.7) \times 10^7$
16 molecule $\text{cm}^{-3} \text{ s}^{-1}$, which can thus be surmised to originate from VOC chemistry. In addition,
17 for both periods, during night time ($J(\text{O}^1\text{D}) \leq 3 \times 10^{-6} \text{ s}^{-1}$), the IPI-LIF-FAGE and the CIMS
18 instruments both measured non-negligible OH concentrations (Hens et al., 2014) where most
19 of the OH production was from unknown sources ($P_{\text{OH}}^{\text{unexplained}} = 1 \pm 0.9 \times 10^6$ molecule cm^{-3}
20 s^{-1} (1σ) and $P_{\text{OH}}^{\text{unexplained}} = 1.7 \pm 0.7 \times 10^7$ molecule $\text{cm}^{-3} \text{ s}^{-1}$ (1σ) for low and high reactivity,
21 respectively). Our hypothesis is that ozonolysis of VOC could represent the missing OH
22 source. Indeed, formation of OH from oxidation of unsaturated VOC has been shown to be an

1 important source of OH in winter, indoors and during night time (Paulson and Orlando,
 2 1996;Geyer et al., 2003;Ren et al., 2003;Heard et al., 2004;Harrison et al., 2006;Johnson and
 3 Marston, 2008;Shallcross et al., 2014). As OH formation from ozonolysis proceeds through
 4 Criegee intermediates (Fig. 2), we can attempt to estimate a SCI concentration from the OH
 5 budget. First, we estimate from the unexplained OH reactivity $P_{OH}^{unexplained}$ a so-called
 6 unexplained O₃ reactivity, $\Sigma(k_{VOC+O_3} \times [VOC_{unidentified}])$, assuming a certain yield of OH from
 7 ozonolysis of unsaturated VOC. Next, we estimate a yield of SCI based on available literature
 8 data, and finally we combine both to estimate the SCI concentration required to close the OH
 9 budget. In contrast to the previous estimates, an average value is obtained for the SCI, and
 10 not a time series, as we start from the average $P_{OH}^{unexplained}$, as reported in Hens et al. (2014).

11 Assuming that all unexplained OH production, $P_{OH}^{unexplained}$, comes from VOC ozonolysis with
 12 a certain OH yield Y_{OH} we obtain:

$$13 \quad P_{OH}^{unexplained} = k_{voc+O_3} \times [VOC_{unidentified}] \times [O_3] \times Y_{OH} \quad (5)$$

14 where $VOC_{unidentified}$ includes the VOC not considered in the OH budget performed by Hens
 15 et al. (2014), i.e. the VOC causing the unknown OH reactivity discussed above. The average
 16 total OH yield from ozonolysis, Y_{OH} , is estimated at about 0.6 based on observed OH yields
 17 from the literature (Atkinson et al., 2006). OH formation from ozonolysis occurs through two
 18 channels (Fig. 2): prompt formation by the decomposition of chemically activated CI^* , and
 19 delayed OH by formation of SCI followed by their thermal decomposition; there are also
 20 product channels not yielding OH. The prompt yield of OH, $Y_{OH}^{CI^*}$ is estimated at ~ 0.4 from
 21 SCI scavenging experiments (Atkinson et al., 2004); the remaining yield Y_{OH}^{SCI} is then formed
 22 from SCI, where $Y_{OH} = Y_{OH}^{CI^*} + Y_{OH}^{SCI}$ and hence $Y_{OH}^{SCI} \approx 0.2$.

1 We adopt a value for Y_{SCI} of 0.4, as argued in section 3.2. The SCI formed do not all
 2 decompose to OH, e.g. *anti*-CI tend to form esters instead. We label all SCI able to yield OH
 3 as SCI_{syn} , without mandating a speciation but following the observation that *syn*-CI usually
 4 yield OH through the vinylhydroperoxide channel. The total SCI yield is then divided into a
 5 fraction, Y_{syn} , forming SCI_{syn} , and the remainder, Y_{anti} , forming non-OH-generating SCI. Little
 6 information is available on the $Y_{syn}:Y_{anti}$ ratio, with only a few theoretical calculations on
 7 smaller alkenes and a few monoterpenes (Rathman et al., 1999;Fenske et al., 2000b;Kroll et
 8 al., 2002;Nguyen et al., 2009b;Nguyen et al., 2009a). For most of these compounds the ratio
 9 of *syn*- to *anti*-SCI is between 0.2 and 1.0 (Rickard et al., 1999) where a larger fraction of
 10 *syn*- to *anti*-SCI, or vice versa, will depend on the single alkene. As there is no information
 11 available for the VOC included in this study, we estimate the ratio of Y_{syn} to Y_{anti} as 1:1. This
 12 number avoids overestimating the impact of SCI in the OH production and, using the *syn* to
 13 *anti* range indicated above, would cause a variation in the final [SCI] estimate of maximum
 14 20 %, (see eq. 7 and Figure 3) well below the total uncertainty of the result.

15 The production of OH from SCI_{syn} formed from VOC not included in the OH budget is then
 16 $k_{OH} \times [SCI_{syn}]$, where we estimate $k_{OH} \approx 20 \text{ s}^{-1}$ as measured by Novelli et al. (2014b) for *syn*-
 17 CH_3CHOO , and where the steady state concentration of the SCI_{syn} , $[SCI_{syn}]$, is determined by
 18 the ratio of the formation processes and the sum $L_{SCI_{syn}}$ of the loss processes already defined
 19 above:

$$20 \quad [SCI_{syn}] = \frac{k_{voc+O_3} \times [VOC_{unidentified}] \times [O_3] \times Y_{SCI} \times Y_{syn}}{L_{SCI_{syn}}} \quad (6)$$

21 Merging the above equations, expressing the measured OH production from unknown
 22 sources as the sum of direct OH production from CI^* and indirect from SCI_{syn} , we obtain:

$$P^{unexplained} = k_{voc+O_3} \times [VOC_{unidentified}] \times [O_3] \times \left(Y_{OH}^{CI^*} + Y_{SCI} \times Y_{syn} \times \frac{k_{OH}}{L_{SCI_{syn}}} \right) \quad (7)$$

The measured $P_{OH}^{unexplained}$ and $[O_3]$, and the estimates of the other parameters allow us to calculate the factor $k_{voc+O_3} \times [VOC_{unidentified}]$. Substituting this factor into Eq. 6 yields an estimate of the steady state concentration of SCI_{syn} . With a value for $P_{OH}^{unexplained}$ of 1×10^6 molecules $cm^{-3} s^{-1}$ as observed for low reactivity episodes and at night during HUMPPA, a steady state concentration of SCI_{syn} of $(2 \pm 2) \times 10^4$ molecules cm^{-3} is calculated. For high reactivity episodes during HUMPPA-COPEC 2010, the missing $P_{OH}^{unexplained}$ of 2×10^7 molecules $cm^{-3} s^{-1}$ results in a SCI concentration of $(4 \pm 4) \times 10^5$ molecules cm^{-3} . To obtain the total SCI concentration, we then need to add the non-OH-producing SCI. Here we assume that these are mostly *anti*-SCI or H_2COO , both of which react rather quickly with H_2O or $(H_2O)_2$ (Taatjes et al., 2013;Chao et al., 2015;Lewis et al., 2015), and that their contribution can be neglected. We thus obtain that $[SCI] \approx [SCI_{syn}]$. To this we add the SCI concentration calculated from the measured unsaturated VOC (section 3.2), $(5 \pm 4) \times 10^3$ molecules cm^{-3} , to obtain the SCI formed from all VOC.

For HOPE 2012 it is difficult to accurately derive an OH budget due to the lack of information on the HONO concentration, which can represent an important primary source of OH. A detailed analysis of the OH production and loss during the campaign thus requires a detailed model study to derive HONO concentrations, which is outside the scope of this paper. Hence, an estimate on the SCI from a possible missing OH production rate during the HOPE 2012 campaign is not included here.

Equation 7, for a given set of yields, unimolecular decomposition rates and SCI losses, allows the estimate of the relative contribution of SCI and Cl^* to the total production rate of OH from the ozonolysis of VOC. With the yields considered in this study and for a unimolecular decomposition rate of SCI into OH of 20 s^{-1} , the SCI would contribute up to 12 % to the total formation of OH from ozonolysis of VOC in both environments. This indicates that the SCI do not have a large impact in the production of OH radicals and at the same time emphasizes how important a realistic estimate of VOC concentration is for modeling the OH radical as already underlined by (Hens et al., 2014).

3.5 Robustness of the [SCI] estimates

Figure 3 summarises the steady state concentration of SCI calculated on the basis of the H_2SO_4 budget, the measured unsaturated VOC concentration and OH reactivity (R), and the OH budget for the HUMPPA-COPEC 2010 and HOPE 2012 campaigns. By considering the lower and the highest values estimated from the measured VOC and from the missing H_2SO_4 oxidant for both campaigns, respectively, the steady state concentration of SCI is calculated to be between 5×10^3 and $2 \times 10^6 \text{ molecules cm}^{-3}$ for the boreal forest environment during the HUMPPA-COPEC 2010 campaign and between 7×10^3 and $1 \times 10^6 \text{ molecules cm}^{-3}$ for rural Germany during the HOPE 2012 campaign (Table 2). The SCI concentrations calculated using these approaches represent a best-effort estimate made for the environments studied here based on the available data; due to the many uncertainties related to the chemistry of SCI both in production and loss processes these estimates span about two orders of magnitude.

The estimate of the SCI concentration from the sulfuric acid budgets relies on the rate of oxidation of SO_2 to H_2SO_4 . As indicated in section 3.1, two significantly different rate coefficients for the reaction of SCI with SO_2 are currently available. One coefficient is high, $\sim 3.3 \pm 2 \times 10^{-11} \text{ cm}^3 \text{ molecule}^{-1} \text{ s}^{-1}$, while the other is several orders of magnitude lower, $5 \times$

1 $10^{-13} \text{ cm}^3 \text{ molecule}^{-1} \text{ s}^{-1}$. Justifications of the differences in the values due to the diverse
2 procedures, i.e. direct detection of SCI + SO₂ for the high rate coefficient and detection of
3 H₂SO₄ for the lower one, are difficult, while recent measurements tend to agree with the
4 highest value. This casts doubts on the highest obtained SCI concentrations of $\sim 10^6$
5 molecules cm⁻³. In addition, the remaining three estimates strongly depend on the yield of
6 SCI, $k_{\text{VOC}+\text{O}_2}$ and $L_{\text{SCI}_{\text{syn}}}$. Among these, the parameter with the highest uncertainty is the loss
7 rate of *syn*-SCI, $L_{\text{SCI}_{\text{syn}}}$, as it is based on relatively few studies, which report large differences
8 between the observations. In this study, a value of 40 s⁻¹ and of 32 s⁻¹, based on previous
9 model analysis (Novelli et al., 2014b), for the HUMPPA-COPEC 2010 and HOPE 2012
10 campaigns respectively, were used. Recent work (Smith et al., 2016; Fang et al., 2016a; Long
11 et al., 2016) suggests a faster unimolecular decomposition rate for the acetone oxide Criegee
12 intermediate, exceeding 10² s⁻¹ in ambient conditions. It is currently not clear whether this
13 rate applies to more substituted SCI as formed from monoterpenes but the use of these higher
14 decomposition rate in the model by (Novelli et al., 2014b) would result in a total $L_{\text{SCI}_{\text{syn}}}$ of \sim
15 110 s⁻¹. This loss rate would decrease the estimated SCI concentration by almost a factor of 3,
16 closer to the lower estimates not exceeding 10⁵ molecule cm⁻³; this also casts doubt on the
17 highest estimates given in Figure 3. Therefore, an average estimated SCI concentration of
18 about 5×10^4 molecules cm⁻³, with an order of magnitude uncertainty, is considered more
19 appropriate for both campaigns.

20

21 **4 The source of the OH background signal**

22 In this section we examine the background OH signal, OH_{bg} (Novelli et al., 2014b) measured
23 during the two field campaigns discussed in the previous sections. In particular, we examine
24 if this signal is consistent with the SCI chemistry and concentrations indicated above.

4.1 Correlation of OH_{bg} with temperature

The time series of the background OH signal measured during the HUMPPA-COPEC 2010 and HOPE 2012 campaigns are shown together with temperature and J(O¹D) values in Fig. 4. Increases and decreases in the OH_{bg} signal follow the temperature changes. During the HUMPPA-COPEC 2010 campaign the OH_{bg} shows a strong correlation with temperature (Fig. 5) with a correlation coefficient $R = 0.8$ for the exponential fit. The exponential dependency with temperature is in agreement with data shown by Di Carlo et al. (2004) for the unexplained OH reactivity and indicates that the species responsible for the OH_{bg} strongly correlate with emission of biogenic VOC (BVOC) such as monoterpenes and sesquiterpenes, which have been shown to also exponentially depend on temperature (Guenther et al., 1993; Duhl et al., 2008; Hakola et al., 2003). This suggests that OH_{bg} is directly related to BVOC chemistry. The relationship between OH_{bg} and temperature during the HOPE 2012 campaign is less obvious. It is possible to observe a weakly exponential correlation between the two ($R = 0.51$, Fig. SI-10) but there is very large scatter in the data. It is worthwhile to underline the differences between the two environments. The forest in Finland is essentially pristine and BVOC dominated while in southern Germany a large fraction of non-biogenic VOC was observed. The lack of a clear exponential correlation between OH_{bg} and temperature during the HOPE 2012 campaign could suggest different precursors or a different origin for the OH_{bg} within the two environments.

During both campaigns a negligible correlation, $R = 0.2$, was observed between background OH and J(O¹D). This suggests that the OH_{bg} does not primarily originate from photolabile species.

4.2 Correlation of OH_{bg} with unexplained OH reactivity

As described in section 3.3, during the HUMPPA-COPEC 2010 campaign high average OH reactivity was observed ($\sim 9 \text{ s}^{-1}$), of which between 60 % and 90 % cannot be explained by the loss processes calculated from the measured species (Nölscher et al., 2012). A large unexplained fraction of the reactivity has often been observed, especially in forested environments (Di Carlo et al., 2004; Sinha et al., 2008; Edwards et al., 2013) indicating a large fraction of undetected BVOC and/or secondary oxidation products. The OH_{bg} shows some correlation with the measured unexplained OH reactivity at 18 m, for the period on the ground ($R = 0.4$), and the measured unexplained OH reactivity at 24 m, for the period on the tower ($R = 0.4$) (Fig. 6). If we consider only night time data, i.e. $J(\text{O}^1\text{D}) \leq 3 \times 10^{-6} \text{ s}^{-1}$ (Hens et al., 2014), we obtain better agreement between the two datasets for both ground and tower periods. During the night a large fraction of observed OH production (section 3.4) could not be explained, which can tentatively be attributed to formation of OH from ozonolysis of BVOC, suggesting that the background OH could be related to such a process. Correlation between the OH_{bg} and the OH reactivity was also observed in a study by Mao et al. (2012) in a Ponderosa pine plantation (California, Sierra Nevada Mountains) dominated by isoprene where even higher OH reactivity was observed ($\sim 20 \text{ s}^{-1}$).

During the HOPE 2012 campaign such a correlation with the unexplained OH reactivity was not observed ($R = 0.1$). The OH reactivity was, on average, 3 times less than during the campaign in Finland and, as shown in section 3.3, of which 50 % can be explained by reaction of OH with methane, formaldehyde, acetaldehyde, inorganic compounds (NO_x, SO₂, CO) and anthropogenic VOC. On average only 17 % of the OH reactivity is caused by reaction of OH with BVOC in this environment (Fig SI-8), dropping to 10 % during the night. The unexplained OH reactivity is not influenced by distinguishing between day and

night time data suggesting a small contribution of non-measured BVOC. As this site is more strongly affected by anthropogenic emissions (Table SI-2) compared to the site in Finland, assuming that the OH_{bg} originates from BVOC driven chemistry, a lack of correlation between OH_{bg} and OH reactivity can be expected.

4.3 Correlation of OH_{bg} with ozonolysis chemistry

During the HUMMPA-COPEC 2010 campaign a high correlation with O_3 , $R = 0.7$ (Fig. SI-11), indicates that background OH likely originates from ozonolysis processes. A comparison of background OH with the product of ozone concentration, measured unsaturated VOC concentration and their ozonolysis rate coefficient does not show the same relationship. No correlation ($R = 0.05$) is found by using the measured BVOC concentrations (Table SI-1). As most of the OH reactivity remains unexplained, with measured BVOC comprising less than 10 % of the measured OH reactivity (Fig SI-6, Table SI-2), the lack of correlation could suggest that the VOC responsible for the formation of SCI detected by the HORUS instrument are likely part of the large fraction of unmeasured species to which a correlation was reported in the previous section.

During HOPE 2012 a weak correlation was observed between background OH and ozone ($R = 0.5$, fig. SI-12).

This campaign, from July 10th to August 19th 2012, encompasses a time period, from 1st to 3rd of August 2012, which was characterized by tree cutting in the vicinity of the measurement site. During this period a significantly larger fraction of unexplained OH reactivity, up to 40 % (Fig. SI-13), was observed. The relative contribution of measured BVOC and inorganic compounds did not change, while the presence of unidentified BVOC emitted from the trees

1 as a result of the stress induced on the plants from the cutting activity, caused the larger
2 fraction of unexplained reactivity. Figure 7 shows the correlation between OH_{bg} and the
3 product $k_{\text{O}_3}[\text{VOC}][\text{O}_3]$ of measured unsaturated VOC concentration (Table SI-1), $[\text{O}_3]$ and
4 the relevant ozonolysis rate coefficients. In red are depicted the data points belonging to the
5 tree cutting period, which naturally correspond to a larger OH_{bg} concentration for similar
6 concentrations of measured VOC during the rest of the campaign, as the additional
7 contribution from the non-identified BVOC is neglected. The overall correlation appears to
8 be pretty poor in particular due to the few points scattering in the lower right corner. These
9 points all belong to three consecutive days, from 26th to 28th of July, which were
10 characterised by high temperature and large concentrations of BVOC (Table SI-3). As
11 noticeable in Figure 4, during those three days the OH_{bg} strongly deviates from the
12 temperature trends and reaches lower values. At present, the reason for such a low
13 concentration of OH_{bg} , during a period which should favour its formation if it originates from
14 SCI, is unclear. The instrument was left unattended at the site and the drop in the quality of
15 the signals required its shutdown on the evening of the 28th of July. However, as no evidence
16 was found to suggest an error in the data the points have not been omitted. Excluding that
17 period yields a correlation factor of $R = 0.65$. The correlation line intercept could arise for a
18 number of reasons. Unmeasured components of the OH reactivity (i.e. unspiciated VOCs)
19 are not accounted for in the calculation, and doing so would shift the data to higher $[\text{VOC}]$,
20 decreasing the positive intercept. This is also consistent with a higher intercept for the cutting
21 tree period where a larger unexplained OH reactivity was observed. It is also conceivable that
22 the intercept is in part due to an additional, non-ozonolysis source of background OH. One
23 candidate for the night time periods could be NO_3 as found in the work by Fuchs et al. (2016).
24 Unfortunately, there was no measurement of the NO_3 radical during the HOPE 2012

campaign, but based on previous studies at the site (Handisides et al., 2003), a concentration up to 14 pptv of NO_3 could be present and could have a detectable impact.

Apart from the possible partial origin of OH_{bg} from NO_3 or other interferences, there are also indications that the background OH could originate from ozonolysis of unsaturated biogenic compounds. The correlation analysis requires that all VOCs are accounted for, and omitting large contributions from unspiciated VOCs, as evidenced e.g. by OH reactivity measurements, can be expected to reduce the correlation as observed in the case of HUMPPA-COPEC 2010. The reason for the lack of correlation during the period from 26th to 28th July 2012 during HOPE-2012 characterised by large BVOC emissions remains unclear.

4.4 Correlation of OH_{bg} with $\text{P}(\text{H}_2\text{SO}_4)_{\text{unex}}$

During both campaigns, measurements of H_2SO_4 , SO_2 , OH and CS (condensation sink) were performed allowing the calculation of the sulfuric acid budget in the gas phase. As shown by Mauldin III et al. (2012), during the HUMPPA-COPEC 2010 campaign the well-known SO_2 oxidation process by OH (Wayne, 2000) (Eq. 1) was not sufficient to explain the measured concentration of H_2SO_4 . As shown in section 3.1, half of the production rate of H_2SO_4 , $\sim 1 \times 10^4$ molecules $\text{cm}^{-3} \text{ s}^{-1}$, cannot be explained by reaction with OH radicals (Fig. 8). The missing oxidant is assumed to be SCI, as discussed in section 3.1, because of their fast reaction rate with SO_2 . As our hypothesis about the origin of the OH_{bg} supports this assumption, we compared the $[\text{H}_2\text{SO}_4]_{\text{unex}}$ observed during the HUMPPA-COPEC 2010 campaign with the OH_{bg} multiplied by SO_2 for the ground-based period when the instruments (HORUS and CIMS) measured side-by-side (Fig. 9). The two datasets indicate a correlation

1 coefficient of $R = 0.6$ suggesting that whichever species is responsible for the oxidation of
2 SO_2 is related to the formation of OH within the HORUS instrument.
3 Note that for the HOPE 2012 campaign the same budget calculation shows only a small
4 fraction (10 %) of unexplained H_2SO_4 production rate (Fig. 1).
5 Assuming SCI to be the unknown SO_2 oxidant, the results observed in both campaigns are in
6 agreement with the modeling study by Boy et al. (2013), who analyzed measurements at the
7 same sites described in this study. Similar to our result, they found a larger contribution of
8 SCI in the formation of H_2SO_4 for the boreal forest compared to rural Germany. As the OH
9 concentration differs by, on average, less than 50 % between the two environments, a similar
10 concentration of SCI in HOPE to that calculated for HUMPPA-COPEC 2010 would
11 contribute up to 30 % in the formation of H_2SO_4 . However, the H_2SO_4 budget during this
12 campaign can approximately be closed by only considering the measured OH concentrations,
13 suggesting that the concentration of SCI in this environment is smaller than that during the
14 HUMPPA-COPEC 2010 campaign. This is consistent with the calculation in section 3 based
15 on the smaller reactivity and hence smaller VOC concentration in this environment

16 **4.5 Scavenging experiments**

17 A series of scavenging tests of the OH_{bg} was performed during the HOPE 2012 campaign to
18 help identify the interfering species. SO_2 was chosen as scavenger for the species causing the
19 OH_{bg} , as it has been shown in several laboratory studies to react quickly with SCI ($k \sim 3.3 \times$
20 $10^{-11} \text{ cm}^3 \text{ molecule}^{-1} \text{ s}^{-1}$) mostly independently of their structure (Taates et al., 2014). The
21 injection of SO_2 was performed through the IPI system (Novelli et al., 2014a) together with
22 an OH scavenger. First the OH scavenger propane was injected within IPI to remove the
23 atmospheric OH; subsequently, SO_2 was injected in addition to the OH scavenger (Fig. 10).
24 The concentration of SO_2 is small enough not to scavenge SCI inside the low pressure section

1 of the instrument, nor is it additionally removing atmospheric OH within the IPI system as
2 the lifetime of OH by reaction with SO₂ is 200 times that of propane. With the addition of
3 SO₂ (1×10^{13} molecules cm⁻³ in the sampled air) it is possible to suppress the OH_{bg} signal
4 from the instrument to within the zero noise, indicating that the OH_{bg} signal originates from
5 an SCI-like species that reacts with SO₂ and decomposes unimolecularly to OH.

7 **4.6 SCI as a source of background OH**

8 During the HUMPPA-COPEC 2010 campaign the background OH showed a strong
9 exponential relationship with temperature ($R = 0.8$) and it correlates with unexplained OH
10 reactivity ($R = 0.5$), which suggests correlation with BVOC, with ozone ($R = 0.7$), and also
11 with the P(H₂SO₄)_{unex} ($R = 0.6$). During the HOPE 2012 campaign a weak exponential
12 correlation with temperature was recognized ($R = 0.5$) but no correlation was observed with
13 OH reactivity. The OH_{bg} correlated with the product of ozone and unsaturated VOC for most
14 of the campaign ($R = 0.6$) although not for a period of three days at the end of July with
15 partly higher BVOC-O₃ turnover. In addition, during HOPE 2012 the OH_{bg} signal was
16 scavenged by the addition of SO₂.

17 All evidence presented indicates that substantial parts of the OH_{bg} originate from a species
18 formed during the ozonolysis of unsaturated VOC that decomposes into OH, is removable by
19 SO₂ and, if present in a significant concentration, increases the H₂SO₄ production. We are
20 currently not aware of any chemical species, other than SCI, known to oxidise SO₂ at a fast
21 enough rate and also decompose into OH. In addition, HORUS was shown to be sensitive to
22 the OH formed after unimolecular decomposition of SCI in the low-pressure region of the
23 instrument (residence time 2 ms) in controlled laboratory studies (Novelli et al., 2014b).

1 During the HUMPPA-COPEC 2010 campaign, the correlation with OH reactivity improved
2 when considering only data during night time, the period during which a higher fraction of
3 the production rate of OH could not be accounted for (Hens et al., 2014). Indeed, during the
4 night recycling via $\text{HO}_2 + \text{NO}$ is low due to the negligible NO concentration, therefore a
5 different path of formation of OH is expected. One likely path could be the formation of OH
6 from excited and stabilised CI formed from ozonolysis of unsaturated compounds.

7 The considerations above are all consistent with the hypothesis that OH_{bg} largely originates
8 from unimolecular decomposition of SCI in the field as well as in the laboratory.

9 Attempts to analyse the absolute concentration of SCI based on our OH_{bg} , however, indicates
10 that this hypothesis is not without difficulties. A particular problem is that to date no method
11 is available to produce and quantify a known concentration of a specific SCI conformer,
12 which precludes the absolute calibration of SCI-generated OH. *A priori*, it seems unlikely
13 that the IPI-LIF-FAGE instrument calibration factor for ambient OH, i.e. sampled from
14 outside the instrument through the nozzle, is identical to the sensitivity for OH generated
15 inside. The transmission factor through our nozzle pinhole is currently not known for OH
16 radicals; the calibration factor used for ambient OH accounts for this transmission as well as
17 for e.g. OH losses on the walls, alignment of the white cell, transmission optics, and response
18 of the MCP. These last three factors should affect the OH generated from any interfering
19 species similarly, while wall losses and transmission through the pinhole are different and
20 possibly also differ between SCI conformers. Additionally, different SCI vary in their
21 unimolecular decomposition rates and hence affect calibration by a different time-specific
22 OH yield. For example, theoretical studies (Vereecken and Francisco, 2012) and laboratory
23 experiments (Smith et al., 2016) indicate that acetone oxide will decompose faster than *syn*-
24 acetaldehyde oxide causing the formation of a different amount of OH, which in turn will

1 also be affected by different loss rates in the low pressure segment of the instrument. Thus, it
2 is not possible to convert the internal OH to an absolute SCI concentration since the mixture
3 of SCI is not known. At best one could obtain an "average" sensitivity factor, if one knew the
4 OH_{bg} formed from a series of reference SCI conformers, and if the ambient SCI speciation is
5 known and not too strongly dependent on reaction conditions. To further illustrate the need of
6 a SCI-specific calibration, we try to simply calculate the external [SCI] from the internal
7 OH_{bg} signal strength, calibrated based on the combined experimental and modelling study by
8 Novelli et al. (2014b). For a SCI mixture that behaves identical to syn-CH₃CHOO, the OH_{bg}
9 from the HUMPPA-COPEC 2010 campaign would then indicate an external [SCI] $\geq 2 \times 10^7$
10 molecules cm⁻³, well above the estimates presented in section 3. Moreover, the observed
11 OH_{bg} signal interpreted in this way would imply an ambient OH production exceeding $4 \times$
12 10^8 molecules cm⁻³ s⁻¹, clearly in disagreement with known chemistry, and also inconsistent
13 with our estimates (Table 2). If we assume a faster decomposition rate for the SCI of 200 s⁻¹,
14 a higher fraction of the SCI decomposes in the low-pressure region, i.e. 80 % compared to 25
15 % for $k_{\text{uni}} = 20$ s⁻¹. This leads to a higher OH signal per SCI, and from this a [SCI] of 4×10^6
16 molecules cm⁻³, though the implied ambient OH production would remain significantly too
17 high. Thus, the conversion of the OH signal to an absolute concentration of ambient SCI is
18 not unambiguous without full SCI speciation and knowledge of their chemical kinetics. Note
19 furthermore that these [SCI] estimates would represent a lower limit as we only observe SCI
20 that decompose to OH, whereas e.g. *anti*-SCI convert to acids/esters.

21 In an effort to work towards SCI-specific calibration, we probed the transmission of OH and
22 syn-CH₃CHOO through the nozzles and the low-pressure region in the instrument, with
23 explorative laboratory tests using a traditional nozzle and a molecular beam skimmer nozzle,
24 where the latter has much thinner sidewalls and a significantly narrower gas expansion,

1 strongly reducing wall contact. The laboratory test showed that the OH radical has a 23 %
2 higher transmission through the molecular beam nozzle compared to the traditional nozzle.
3 The *syn*-acetaldehyde oxide did not show any statistical difference in the transmission
4 between the two nozzles. This indicates that (a) SCI and OH have a different transmission
5 efficiency and most likely different wall losses, underlining that the OH calibration factor is
6 not applicable to SCI for ambient measurements, and (b) that the calibration factor for OH
7 obtained for ambient OH alone does not allow the quantification of the absolute OH
8 concentration in the low-pressure section of the FAGE instrument. This is the fundamental
9 reason why the earlier simple estimate of [SCI] and OH production leads to strong over-
10 estimations.

11 In addition to the above effects, one should also consider that OH-production from SCI in the
12 low-pressure section might be catalysed to proceed at rates beyond their ambient counterpart,
13 biasing our interpretation of their ambient fate. The catalysis might involve wall-induced
14 isomerisation of the higher-energy *anti*-SCI to the more stable, OH-producing *syn*-SCI,
15 which would artificially increase the *syn:anti* ratio. Another possibility is the evaporation of
16 clusters stabilizing the SCI, as it is known that SCI efficiently form complexes with many
17 compounds, including water, acids, alcohols, hydroperoxides, HO_x radicals, etc. (Vereecken
18 and Francisco, 2012). Redissociation of secondary ozonides (SOZ) seems less important,
19 except perhaps the SOZ formed with CO₂ (Aplincourt and Ruiz-López, 2000), which has no
20 alternative accessible unimolecular channels. At present, insufficient (if any) information is
21 available to assess the impact of such catalysis.

22 Taking into account the factors considered above, and assuming that the estimates for the SCI
23 concentration in both environments are correct, it appears unlikely that SCI are responsible
24 for such a large OH_{bg} signal as observed by the HORUS instrument. If SCI were to be solely

1 responsible for the OH_{bg} signal, the HORUS instrument would need to be far more sensitive
2 to the detection of SCI than to the detection of OH radicals by, for example, pinhole losses
3 that are 100 times smaller for SCI than for OH radicals. The evident discrepancy between the
4 qualitative evidence in support of the SCI hypothesis and the current quantitative difficulty in
5 reconciling the OH_{bg} signal with the estimated ambient concentration of SCI does not allow
6 an unequivocal identification of the origin of the OH_{bg} within our system. It cannot be
7 excluded that multiple species are contributing to the OH_{bg} signal. NO₃ chemistry during
8 night time has been identified as a possible source of OH_{bg} in the LIF-FAGE instrument of
9 the FZ-Jülich (Fuchs et al., 2016). However, in the case of the large observed night time OH_{bg}
10 concentrations during HUMPPA-COPEC 2010, the measured night time NO₃ concentrations
11 were below 1 ppt and therefore too small to explain the observed OH_{bg}.

12

13 **5 Conclusions**

14 We estimated a steady state concentration of SCI for the HUMPPA-COPEC 2010 and the
15 HOPE 2012 campaigns based on a large dataset. Starting from four different approaches, i.e.
16 based on unaccounted (i.e. non-OH) H₂SO₄ oxidant, measured VOC concentrations,
17 unexplained OH reactivity or unexplained production rates of OH, we estimated the
18 concentration of SCI to be between $\sim 10^3$ and $\sim 10^6$ molecules cm⁻³. The highest values in
19 this range are linked to an assumed low rate coefficient for SCI + SO₂ of 5×10^{-13} cm³
20 molecule⁻¹ s⁻¹ (see section 3.1), which is at odds with a larger body of more direct
21 measurements on this rate coefficient. Hence, higher SCI values appear to be relatively less
22 likely. We thus obtain an average SCI concentration of about 5×10^4 molecules cm⁻³, with an
23 order of magnitude uncertainty, for both campaigns. At such concentrations, SCI are
24 expected to have a significant impact on H₂SO₄ chemistry during the HUMPPA-COPEC

1 2010 campaign while during the HOPE 2012 campaign their impact is much smaller and
2 possibly negligible. Additionally, it was shown that, based on the yields and unimolecular
3 decomposition rate applied in this study, SCI do not have a large impact on the OH
4 production compared to the direct OH generation from ozonolysis of unsaturated VOC.
5 During both campaigns, the IPI-LIF-FAGE instrument detected an OH background signal
6 that originates from decomposition of one or more species inside the low pressure region of
7 the instrument. The source compound of the OH_{bg} was shown to be unreactive towards
8 propane but to be removed by SO₂, and a relationship was found with the unaccounted H₂SO₄
9 production rate. It correlates with temperature in the same way as the emission of terpenes
10 and, in most but not all measurements periods, with the product of unsaturated VOC and
11 ozone as well as with the OH reactivity. While it is not possible at the moment to
12 unequivocally state that OH_{bg} originates from stabilised Criegee intermediates, the
13 observations are consistent with known SCI chemistry. The contribution of SCI to the
14 observed OH_{bg} cannot be quantified until a calibration scheme for SCI in the IPI-FAGE
15 system has been developed.

16 The predicted SCI concentrations derived in this study are low, likely not exceeding 10⁵
17 molecule cm⁻³, therefore, the presence of SCI is unlikely to have a large impact on
18 atmospheric chemistry; the main exception appears to be H₂SO₄ production in selected
19 environments.

20

21 **Acknowledgements**

22 LV was supported by the Max Planck Graduate Centre (MPGC) with the Johannes
23 Gutenberg-Universität Mainz.

1 Work during HUMPPA-COPEC was supported by the Hyytiälä site engineers and staff.
2 Support of the European Community Research Infrastructure Action under the FP6
3 "Structuring the European Research Area" Programme, EUSAAR Contract No RII3-CT-
4 2006-026140 is gratefully acknowledged. The HUMPPA-COPEC 2010 campaign
5 measurements and analyses were supported by the ERC Grant ATMNUCLE (project No
6 227463), Academy of Finland Centre of Excellence program (project No 1118615), ,
7 Academy of Finland Centre of Excellence in Atmospheric Science – From Molecular and
8 Biological processes to The Global Climate' (ATM), 272041, the European integrated project
9 on Aerosol Cloud Climate and Air Quality Interactions EUCAARI (project No 036833-2),
10 the EUSAAR TNA (project No 400586), and the IMECC TA (project No 4006261).

11 The work during HOPE 2012 was supported by the scientists and staff of DWD
12 Hohenpeißenberg whom we would like to thank for providing the "platform" and opportunity
13 to perform such campaign. In particular, we thank, Anja Werner, Jennifer Englert and Katja
14 Michl for the VOC measurements, Stephan Gilge for the trace gases measurements and
15 Georg Stange for running the CIMS.

16 We also would like to thank Markus Rudolf for much technical support and guidance, Eric
17 Regelin and Umar Javed for the numerous scientific discussions, Petri Keronen for providing
18 meteorological and trace gas concentration data from Hyytiälä during the HUMPPA-COPEC
19 2010 and Thorsten Berndt for providing the data to re-evaluate the rate coefficient between
20 SCI and SO₂.

21

22 **References**

- 23 Aalto, P., Hämeri, K., Becker, E. D. O., Weber, R., Salm, J., Mäkelä, J. M., Hoell, C.,
24 O'Dowd, C. D., Karlsson, H., Hansson, H.-C., Väkevä, M., Koponen, I. K., Buzorius, G., and
25 Kulmala, M.: Physical characterization of aerosol particles during nucleation events, *Tellus*
26 *B*, 53, 344-358, 10.1034/j.1600-0889.2001.530403.x, 2001.
- 27 Ahrens, J., Carlsson, P. T., Hertl, N., Olzmann, M., Pfeifle, M., Wolf, J. L., and Zeuch, T.:
28 Infrared detection of Criegee intermediates formed during the ozonolysis of beta-pinene and
29 their reactivity towards sulfur dioxide, *Angew Chem Int Ed Engl*, 53, 715-719,
30 10.1002/anie.201307327, 2014.

1 Amédéo, D.: Atmospheric measurements of OH and HO₂ radicals using FAGE :
2 Development and deployment on the field, Université Lille1 - Sciences et Technologies,
3 Tokyo Metropolitan University, 2012.

4 Anglada, J. M., Bofill, J. M., Olivella, S., and Solé, A.: Unimolecular Isomerizations and
5 Oxygen Atom Loss in Formaldehyde and Acetaldehyde Carbonyl Oxides. A Theoretical
6 Investigation, *J Am Chem Soc*, 118, 4636-4647, 10.1021/ja953858a, 1996.

7 Anglada, J. M., Gonzalez, J., and Torrent-Sucarrat, M.: Effects of the substituents on the
8 reactivity of carbonyl oxides. A theoretical study on the reaction of substituted carbonyl
9 oxides with water, *Phys Chem Chem Phys*, 13, 13034-13045, 2011.

10 Anglada, J. M., and Sole, A.: Impact of water dimer on the atmospheric reactivity of carbonyl
11 oxides, *Phys Chem Chem Phys*, 10.1039/C6CP02531E, 2016.

12 Aplin-court, P., and Ruiz-López, M. F.: Theoretical Investigation of Reaction Mechanisms for
13 Carboxylic Acid Formation in the Atmosphere, *J Am Chem Soc*, 122, 8990-8997,
14 10.1021/ja000731z, 2000.

15 Atkinson, R., Baulch, D. L., Cox, R. A., Crowley, J. N., Hampson, R. F., Hynes, R. G.,
16 Jenkin, M. E., Rossi, M. J., and Troe, J.: Evaluated kinetic and photochemical data for
17 atmospheric chemistry: Volume I - gas phase reactions of Ox, HOx, NOx and SOx species,
18 *Atmos. Chem. Phys.*, 4, 1461-1738, 10.5194/acp-4-1461-2004, 2004.

19 Atkinson, R., Baulch, D. L., Cox, R. A., Crowley, J. N., Hampson, R. F., Hynes, R. G.,
20 Jenkin, M. E., Rossi, M. J., Troe, J., and Subcommittee, I.: Evaluated kinetic and
21 photochemical data for atmospheric chemistry: Volume II - gas phase reactions of organic
22 species, *Atmos. Chem. Phys.*, 6, 3625-4055, 10.5194/acp-6-3625-2006, 2006.

23 Berndt, T., Jokinen, T., Mauldin, R. L., Petaja, T., Herrmann, H., Junninen, H., Paasonen, P.,
24 Worsnop, D. R., and Sipila, M.: Gas-Phase Ozonolysis of Selected Olefins: The Yield of
25 Stabilized Criegee Intermediate and the Reactivity toward SO₂, *J. Phys. Chem. Lett.*, 3, 2892-
26 2896, 10.1021/jz301158u, 2012.

27 Berndt, T., Jokinen, T., Sipilä, M., Mauldin Iii, R. L., Herrmann, H., Stratmann, F., Junninen,
28 H., and Kulmala, M.: H₂SO₄ formation from the gas-phase reaction of stabilized Criegee
29 Intermediates with SO₂: Influence of water vapour content and temperature, *Atmos Environ*,
30 89, 603-612, <http://dx.doi.org/10.1016/j.atmosenv.2014.02.062>, 2014a.

31 Berndt, T., Voigtlander, J., Stratmann, F., Junninen, H., Mauldin Iii, R. L., Sipilä, M.,
32 Kulmala, M., and Herrmann, H.: Competing atmospheric reactions of CH₂OO with SO₂ and
33 water vapour, *Phys Chem Chem Phys*, 16, 19130-19136, 10.1039/c4cp02345e, 2014b.

34 Berresheim, H., Elste, T., Plass-Dülmer, C., Eisele, F. L., and Tanner, D. J.: Chemical
35 ionization mass spectrometer for long-term measurements of atmospheric OH and H₂SO₄,
36 *International Journal of Mass Spectrometry*, 202, 91-109, [http://dx.doi.org/10.1016/S1387-](http://dx.doi.org/10.1016/S1387-3806(00)00233-5)
37 [3806\(00\)00233-5](http://dx.doi.org/10.1016/S1387-3806(00)00233-5), 2000.

38 Birmili, W., Berresheim, H., Plass-Dülmer, C., Elste, T., Gilge, S., Wiedensohler, A., and
39 Uhrner, U.: The Hohenpeissenberg aerosol formation experiment (HAFEX): a long-term
40 study including size-resolved aerosol, H₂SO₄, OH, and monoterpenes measurements, *Atmos.*
41 *Chem. Phys.*, 3, 361-376, 10.5194/acp-3-361-2003, 2003.

42 Boy, M., Mogensen, D., Smolander, S., Zhou, L., Nieminen, T., Paasonen, P., Plass-Dülmer,
43 C., Sipilä, M., Petäjä, T., Mauldin, L., Berresheim, H., and Kulmala, M.: Oxidation of SO₂ by

1 stabilized Criegee intermediate (sCI) radicals as a crucial source for atmospheric sulfuric acid
2 concentrations, *Atmos. Chem. Phys.*, 13, 3865-3879, 10.5194/acp-13-3865-2013, 2013.

3 Buras, Z. J., Elsamra, R. M., Jalan, A., Middaugh, J. E., and Green, W. H.: Direct kinetic
4 measurements of reactions between the simplest Criegee intermediate CH₂OO and alkenes, *J*
5 *Phys Chem A*, 118, 1997-2006, 10.1021/jp4118985, 2014.

6 Chao, W., Hsieh, J.-T., Chang, C.-H., and Lin, J. J.-M.: Direct kinetic measurement of the
7 reaction of the simplest Criegee intermediate with water vapor, *Science*,
8 10.1126/science.1261549, 2015.

9 Chen, L., Wang, W., Wang, W., Liu, Y., Liu, F., Liu, N., and Wang, B.: Water-catalyzed
10 decomposition of the simplest Criegee intermediate CH₂OO, *Theoretical Chemistry*
11 *Accounts*, 135, 1-13, 10.1007/s00214-016-1894-9, 2016.

12 Chhantyal-Pun, R., Davey, A., Shallcross, D. E., Percival, C. J., and Orr-Ewing, A. J.: A
13 kinetic study of the CH₂OO Criegee intermediate self-reaction, reaction with SO₂ and
14 unimolecular reaction using cavity ring-down spectroscopy, *Phys Chem Chem Phys*,
15 10.1039/c4cp04198d, 2015.

16 Criegee, R.: Mechanism of Ozonolysis, *Angew. Chem.-Int. Edit. Engl.*, 14, 745-752,
17 10.1002/anie.197507451, 1975.

18 Di Carlo, P., Brune, W. H., Martinez, M., Harder, H., Leshner, R., Ren, X. R., Thornberry, T.,
19 Carroll, M. A., Young, V., Shepson, P. B., Riemer, D., Apel, E., and Campbell, C.: Missing
20 OH reactivity in a forest: Evidence for unknown reactive biogenic VOCs, *Science*, 304, 722-
21 725, 10.1126/science.1094392, 2004.

22 Donahue, N. M., Drozd, G. T., Epstein, S. A., Presto, A. A., and Kroll, J. H.: Adventures in
23 ozoneland: down the rabbit-hole, *Phys Chem Chem Phys*, 13, 10848-10857,
24 10.1039/c0cp02564j, 2011.

25 Drozd, G. T., and Donahue, N. M.: Pressure Dependence of Stabilized Criegee Intermediate
26 Formation from a Sequence of Alkenes, *J Phys Chem A*, 115, 4381-4387,
27 10.1021/jp2001089, 2011.

28 Drozd, G. T., Kroll, J., and Donahue, N. M.: 2,3-Dimethyl-2-butene (TME) Ozonolysis:
29 Pressure Dependence of Stabilized Criegee Intermediates and Evidence of Stabilized Vinyl
30 Hydroperoxides, *J Phys Chem A*, 115, 161-166, 10.1021/jp108773d, 2011.

31 Duhl, T. R., Helmig, D., and Guenther, A.: Sesquiterpene emissions from vegetation: a
32 review, *Biogeosciences*, 5, 761-777, 10.5194/bg-5-761-2008, 2008.

33 Edwards, P. M., Evans, M. J., Furneaux, K. L., Hopkins, J., Ingham, T., Jones, C., Lee, J. D.,
34 Lewis, A. C., Moller, S. J., Stone, D., Whalley, L. K., and Heard, D. E.: OH reactivity in a
35 South East Asian tropical rainforest during the Oxidant and Particle Photochemical Processes
36 (OP3) project, *Atmos. Chem. Phys.*, 13, 9497-9514, 10.5194/acp-13-9497-2013, 2013.

37 Fang, Y., Liu, F., Barber, V. P., Klippenstein, S. J., McCoy, A. B., and Lester, M. I.:
38 Communication: Real time observation of unimolecular decay of Criegee intermediates to
39 OH radical products, *The Journal of Chemical Physics*, 144, 061102,
40 doi:<http://dx.doi.org/10.1063/1.4941768>, 2016a.

41 Fang, Y., Liu, F., Klippenstein, S. J., and Lester, M. I.: Direct observation of unimolecular
42 decay of CH₃CH₂CHOO Criegee intermediates to OH radical products, *The Journal of*
43 *Chemical Physics*, 145, 044312, doi:<http://dx.doi.org/10.1063/1.4958992>, 2016b.

1 Fenske, J. D., Hasson, A. S., Ho, A. W., and Paulson, S. E.: Measurement of Absolute
2 Unimolecular and Bimolecular Rate Constants for CH₃CHOO Generated by the trans-2-
3 Butene Reaction with Ozone in the Gas Phase, *The Journal of Physical Chemistry A*, 104,
4 9921-9932, 10.1021/jp0016636, 2000a.

5 Fenske, J. D., Kuwata, K. T., Houk, K. N., and Paulson, S. E.: OH Radical Yields from the
6 Ozone Reaction with Cycloalkenes, *The Journal of Physical Chemistry A*, 104, 7246-7254,
7 10.1021/jp993611q, 2000b.

8 Foreman, E. S., Kapnas, K. M., and Murray, C.: Reactions between Criegee Intermediates
9 and the Inorganic Acids HCl and HNO₃: Kinetics and Atmospheric Implications,
10 *Angewandte Chemie International Edition*, n/a-n/a, 10.1002/anie.201604662, 2016.

11 Fuchs, H., Tan, Z., Hofzumahaus, A., Broch, S., Dorn, H. P., Holland, F., K nstler, C.,
12 Gomm, S., Rohrer, F., Schr de, S., Tillmann, R., and Wahner, A.: Investigation of potential
13 interferences in the detection of atmospheric ROx radicals by laser-induced fluorescence
14 under dark conditions, *Atmos. Meas. Tech.*, 9, 1431-1447, 10.5194/amt-9-1431-2016, 2016.

15 Geyer, A., B chmann, K., Hofzumahaus, A., Holland, F., Konrad, S., Kl pfel, T., P tz, H.-
16 W., Perner, D., Mihelcic, D., Sch fer, H.-J., Volz-Thomas, A., and Platt, U.: Nighttime
17 formation of peroxy and hydroxyl radicals during the BERLIOZ campaign: Observations and
18 modeling studies, *Journal of Geophysical Research: Atmospheres*, 108, 8249,
19 10.1029/2001jd000656, 2003.

20 Gilge, S., Plass-D lmer, C., Fricke, W., Kaiser, A., Ries, L., Buchmann, B., and Steinbacher,
21 M.: Ozone, carbon monoxide and nitrogen oxides time series at four alpine GAW mountain
22 stations in central Europe, *Atmos. Chem. Phys.*, 10, 12295-12316, 10.5194/acp-10-12295-
23 2010, 2010.

24 Griffith, S. M., Hansen, R. F., Dusanter, S., Stevens, P. S., Alaghmand, M., Bertman, S. B.,
25 Carroll, M. A., Erickson, M., Galloway, M., Grossberg, N., Hottle, J., Hou, J., Jobson, B. T.,
26 Kammrath, A., Keutsch, F. N., Lefer, B. L., Mielke, L. H., O'Brien, A., Shepson, P. B.,
27 Thurlow, M., Wallace, W., Zhang, N., and Zhou, X. L.: OH and HO₂ radical
28 chemistry during PROPHET 2008 and CABINEX 2009 – Part 1: Measurements and
29 model comparison, *Atmos. Chem. Phys.*, 13, 5403-5423, 10.5194/acp-13-5403-2013, 2013.

30 Griffith, S. M., Hansen, R. F., Dusanter, S., Michoud, V., Gilman, J. B., Kuster, W. C.,
31 Veres, P. R., Graus, M., de Gouw, J. A., Roberts, J., Young, C., Washenfelder, R., Brown, S.
32 S., Thalman, R., Waxman, E., Volkamer, R., Tsai, C., Stutz, J., Flynn, J. H., Grossberg, N.,
33 Lefer, B., Alvarez, S. L., Rappenglueck, B., Mielke, L. H., Osthoff, H. D., and Stevens, P. S.:
34 Measurements of hydroxyl and hydroperoxy radicals during CalNex-LA: Model comparisons
35 and radical budgets, *Journal of Geophysical Research: Atmospheres*, n/a-n/a,
36 10.1002/2015JD024358, 2016.

37 Guenther, A. B., Zimmerman, P. R., Harley, P. C., Monson, R. K., and Fall, R.: Isoprene and
38 monoterpene emission rate variability: Model evaluations and sensitivity analyses, *Journal of*
39 *Geophysical Research: Atmospheres*, 98, 12609-12617, 10.1029/93jd00527, 1993.

40 Hakola, H., Tarvainen, V., Laurila, T., Hiltunen, V., Hell n, H., and Keronen, P.: Seasonal
41 variation of VOC concentrations above a boreal coniferous forest, *Atmos Environ*, 37, 1623-
42 1634, [http://dx.doi.org/10.1016/S1352-2310\(03\)00014-1](http://dx.doi.org/10.1016/S1352-2310(03)00014-1), 2003.

43 Handisides, G. M., Plass-D lmer, C., Gilge, S., Bingemer, H., and Berresheim, H.:
44 Hohenpeissenberg Photochemical Experiment (HOPE 2000): Measurements and

1 photostationary state calculations of OH and peroxy radicals, *Atmos. Chem. Phys.*, 3, 1565-
2 1588, 10.5194/acp-3-1565-2003, 2003.

3 Harrison, R. M., Yin, J., Tilling, R. M., Cai, X., Seakins, P. W., Hopkins, J. R., Lansley, D.
4 L., Lewis, A. C., Hunter, M. C., Heard, D. E., Carpenter, L. J., Creasey, D. J., Lee, J. D.,
5 Pilling, M. J., Carslaw, N., Emmerson, K. M., Redington, A., Derwent, R. G., Ryall, D.,
6 Mills, G., and Penkett, S. A.: Measurement and modelling of air pollution and atmospheric
7 chemistry in the U.K. West Midlands conurbation: Overview of the PUMA Consortium
8 project, *Sci. Total Environ.*, 360, 5-25, <http://dx.doi.org/10.1016/j.scitotenv.2005.08.053>,
9 2006.

10 Hasson, A. S., Ho, A. W., Kuwata, K. T., and Paulson, S. E.: Production of stabilized Criegee
11 intermediates and peroxides in the gas phase ozonolysis of alkenes: 2. Asymmetric and
12 biogenic alkenes, *Journal of Geophysical Research: Atmospheres*, 106, 34143-34153,
13 10.1029/2001jd000598, 2001.

14 Heard, D. E., Carpenter, L. J., Creasey, D. J., Hopkins, J. R., Lee, J. D., Lewis, A. C., Pilling,
15 M. J., Seakins, P. W., Carslaw, N., and Emmerson, K. M.: High levels of the hydroxyl radical
16 in the winter urban troposphere, *Geophys Res Lett*, 31, L18112, 10.1029/2004gl020544,
17 2004.

18 Hens, K., Novelli, A., Martinez, M., Auld, J., Axinte, R., Bohn, B., Fischer, H., Keronen, P.,
19 Kubistin, D., Nölscher, A. C., Oswald, R., Paasonen, P., Petäjä, T., Regelin, E., Sander, R.,
20 Sinha, V., Sipilä, M., Taraborrelli, D., Tatum Ernest, C., Williams, J., Lelieveld, J., and
21 Harder, H.: Observation and modelling of HOx radicals in a boreal forest, *Atmos. Chem.*
22 *Phys.*, 14, 8723-8747, 10.5194/acp-14-8723-2014, 2014.

23 Hoerger, C. C., Werner, A., Plass-Duelmer, C., Reimann, S., Eckart, E., Steinbrecher, R.,
24 Aalto, J., Arduini, J., Bonnaire, N., Cape, J. N., Colomb, A., Connolly, R., Diskova, J.,
25 Dumitrean, P., Ehlers, C., Gros, V., Hakola, H., Hill, M., Hopkins, J. R., Jäger, J., Junek, R.,
26 Kajos, M. K., Klemp, D., Leuchner, M., Lewis, A. C., Locoge, N., Maione, M., Martin, D.,
27 Michl, K., Nemitz, E., O'Doherty, S., Pérez Ballesta, P., Ruuskanen, T. M., Sauvage, S.,
28 Schmidbauer, N., Spain, T. G., Straube, E., Vana, M., Vollmer, M. K., Wegener, R., and
29 Wenger, A.: ACTRIS non-methane hydrocarbon intercomparison experiment in Europe to
30 support WMO-GAW and EMEP observation networks, *Atmos. Meas. Tech. Discuss.*, 7,
31 10423-10485, 10.5194/amtd-7-10423-2014, 2014.

32 Horie, O., Neeb, P., and Moortgat, G. K.: The reactions of the Criegee intermediate
33 CH₃CHOO in the gas-phase ozonolysis of 2-butene isomers, *Int J Chem Kinet*, 29, 461-468,
34 10.1002/(sici)1097-4601(1997)29:6<461::aid-kin8>3.0.co;2-s, 1997.

35 Horie, O., Schäfer, C., and Moortgat, G. K.: High reactivity of hexafluoroacetone toward
36 criegee intermediates in the gas-phase ozonolysis of simple alkenes, *Int J Chem Kinet*, 31,
37 261-269, 10.1002/(sici)1097-4601(1999)31:4<261::aid-kin3>3.0.co;2-z, 1999.

38 Huang, H.-L., Chao, W., and Lin, J. J.-M.: Kinetics of a Criegee intermediate that would
39 survive high humidity and may oxidize atmospheric SO₂, *Proceedings of the National*
40 *Academy of Sciences*, 10.1073/pnas.1513149112, 2015.

41 Jiang, L., Xu, Y.-s., and Ding, A.-z.: Reaction of Stabilized Criegee Intermediates from
42 Ozonolysis of Limonene with Sulfur Dioxide: Ab Initio and DFT Study, *The Journal of*
43 *Physical Chemistry A*, 114, 12452-12461, 10.1021/jp107783z, 2010.

1 Johnson, D., and Marston, G.: The gas-phase ozonolysis of unsaturated volatile organic
2 compounds in the troposphere, *Chemical Society Reviews*, 37, 699-716, 2008.

3 Junninen, H., Lauri, A., Keronen, P., Aalto, P., Hiltunen, V., Hari, P., and Kulmala, M.:
4 Smart-SMEAR: on-line data exploration and visualization tool for SMEAR stations, *Boreal*
5 *Env. Res.*, 14, 447-457, 2009.

6 Kidwell, N. M., Li, H., Wang, X., Bowman, J. M., and Lester, M. I.: Unimolecular
7 dissociation dynamics of vibrationally activated CH₃CHOO Criegee intermediates to OH
8 radical products, *Nat Chem*, advance online publication, 10.1038/nchem.2488
9 [http://www.nature.com/nchem/journal/vaop/ncurrent/abs/nchem.2488.html#supplementary-](http://www.nature.com/nchem/journal/vaop/ncurrent/abs/nchem.2488.html#supplementary-information)
10 [information](http://www.nature.com/nchem/journal/vaop/ncurrent/abs/nchem.2488.html#supplementary-information), 2016.

11 Kroll, J. H., Sahay, S. R., Anderson, J. G., Demerjian, K. L., and Donahue, N. M.:
12 Mechanism of HO_x Formation in the Gas-Phase Ozone-Alkene Reaction. 2. Prompt versus
13 Thermal Dissociation of Carbonyl Oxides to Form OH, *The Journal of Physical Chemistry A*,
14 105, 4446-4457, 10.1021/jp004136v, 2001.

15 Kroll, J. H., Donahue, N. M., Cee, V. J., Demerjian, K. L., and Anderson, J. G.: Gas-Phase
16 Ozonolysis of Alkenes: Formation of OH from Anti Carbonyl Oxides, *J Am Chem Soc*, 124,
17 8518-8519, 10.1021/ja0266060, 2002.

18 Kulmala, M., Maso, M. D., MÄKelä, J. M., Pirjola, L., VÄKevÄ, M., Aalto, P.,
19 Miikkulainen, P., HÄMeri, K., and O'Dowd, C. D.: On the formation, growth and
20 composition of nucleation mode particles, *Tellus B*, 53, 479-490, 10.1034/j.1600-
21 0889.2001.530411.x, 2001.

22 Kurtén, T., Lane, J. R., Jørgensen, S., and Kjaergaard, H. G.: A Computational Study of the
23 Oxidation of SO₂ to SO₃ by Gas-Phase Organic Oxidants, *The Journal of Physical Chemistry*
24 *A*, 115, 8669-8681, 10.1021/jp203907d, 2011.

25 Kuwata, K. T., Hermes, M. R., Carlson, M. J., and Zogg, C. K.: Computational studies of the
26 isomerization and hydration reactions of acetaldehyde oxide and methyl vinyl carbonyl oxide,
27 *J Phys Chem A*, 114, 9192-9204, 10.1021/jp105358v, 2010.

28 Lee, Y.-P.: Perspective: Spectroscopy and kinetics of small gaseous Criegee intermediates,
29 *The Journal of Chemical Physics*, 143, 020901, doi:<http://dx.doi.org/10.1063/1.4923165>,
30 2015.

31 Lewis, T. R., Blitz, M., Heard, D. E., and Seakins, P.: Direct evidence for a substantive
32 reaction between the C1 Criegee radical, CH₂OO, and the water vapour dimer, *Phys Chem*
33 *Chem Phys*, 10.1039/c4cp04750h, 2015.

34 Lin, L.-C., Chang, H.-T., Chang, C.-H., Chao, W., Smith, M. C., Chang, C.-H., Jr-Min Lin,
35 J., and Takahashi, K.: Competition between H₂O and (H₂O)₂ reactions with
36 CH₂OO/CH₃CHOO, *Phys Chem Chem Phys*, 18, 4557-4568, 10.1039/C5CP06446E, 2016.

37 Liu, F., Beames, J. M., Green, A. M., and Lester, M. I.: UV spectroscopic characterization of
38 dimethyl- and ethyl-substituted carbonyl oxides, *J Phys Chem A*, 118, 2298-2306,
39 10.1021/jp412726z, 2014a.

40 Liu, Y., Bayes, K. D., and Sander, S. P.: Measuring rate constants for reactions of the
41 simplest Criegee intermediate (CH₂OO) by monitoring the OH radical, *J Phys Chem A*, 118,
42 741-747, 10.1021/jp407058b, 2014b.

1 Long, B., Bao, J. L., and Truhlar, D. G.: Atmospheric Chemistry of Criegee Intermediates.
 2 Unimolecular Reactions and Reactions with Water, J Am Chem Soc, 10.1021/jacs.6b08655,
 3 2016.

4 Mao, J., Ren, X., Zhang, L., Van Duin, D. M., Cohen, R. C., Park, J. H., Goldstein, A. H.,
 5 Paulot, F., Beaver, M. R., Crounse, J. D., Wennberg, P. O., DiGangi, J. P., Henry, S. B.,
 6 Keutsch, F. N., Park, C., Schade, G. W., Wolfe, G. M., Thornton, J. A., and Brune, W. H.:
 7 Insights into hydroxyl measurements and atmospheric oxidation in a California forest,
 8 Atmos. Chem. Phys., 12, 8009-8020, 10.5194/acp-12-8009-2012, 2012.

9 Martinez, M., Harder, H., Kubistin, D., Rudolf, M., Bozem, H., Eerdeken, G., Fischer, H.,
 10 Klupfel, T., Gurk, C., Konigstedt, R., Parchatka, U., Schiller, C. L., Stickler, A., Williams, J.,
 11 and Lelieveld, J.: Hydroxyl radicals in the tropical troposphere over the Suriname rainforest:
 12 airborne measurements, Atmospheric Chemistry and Physics, 10, 3759-3773, 2010.

13 Mauldin III, R. L., Berndt, T., Sipila, M., Paasonen, P., Petaja, T., Kim, S., Kurten, T.,
 14 Stratmann, F., Kerminen, V. M., and Kulmala, M.: A new atmospherically relevant oxidant
 15 of sulphur dioxide, Nature, 488, 193-196,
 16 [http://www.nature.com/nature/journal/v488/n7410/abs/nature11278.html#supplementary-](http://www.nature.com/nature/journal/v488/n7410/abs/nature11278.html#supplementary-information)
 17 [information](http://www.nature.com/nature/journal/v488/n7410/abs/nature11278.html#supplementary-information), 2012.

18 Newland, M. J., Rickard, A. R., Alam, M. S., Vereecken, L., Munoz, A., Rodenas, M., and
 19 Bloss, W. J.: Kinetics of stabilised Criegee intermediates derived from alkene ozonolysis:
 20 reactions with SO₂, H₂O and decomposition under boundary layer conditions, Phys Chem
 21 Chem Phys, 10.1039/c4cp04186k, 2015a.

22 Newland, M. J., Rickard, A. R., Vereecken, L., Muñoz, A., Ródenas, M., and Bloss, W. J.:
 23 Atmospheric isoprene ozonolysis: impacts of stabilised Criegee intermediate reactions with
 24 SO₂, H₂O and dimethyl sulfide, Atmos. Chem. Phys., 15, 9521-9536, 10.5194/acp-15-9521-
 25 2015, 2015b.

26 Nguyen, T. L., Peeters, J., and Vereecken, L.: Theoretical study of the gas-phase ozonolysis
 27 of beta-pinene (C(10)H(16)), Phys Chem Chem Phys, 11, 5643-5656, 10.1039/b822984h,
 28 2009a.

29 Nguyen, T. L., Winterhalter, R., Moortgat, G., Kanawati, B., Peeters, J., and Vereecken, L.:
 30 The gas-phase ozonolysis of [small beta]-caryophyllene (C₁₅H₂₄). Part II: A theoretical
 31 study, Phys Chem Chem Phys, 11, 4173-4183, 2009b.

32 Nölscher, A. C., Williams, J., Sinha, V., Custer, T., Song, W., Johnson, A. M., Axinte, R.,
 33 Bozem, H., Fischer, H., Pouvesle, N., Phillips, G., Crowley, J. N., Rantala, P., Rinne, J.,
 34 Kulmala, M., Gonzales, D., Valverde-Canossa, J., Vogel, A., Hoffmann, T., Ouwersloot, H.
 35 G., Vilà-Guerau de Arellano, J., and Lelieveld, J.: Summertime total OH reactivity
 36 measurements from boreal forest during HUMPPA-COPEC 2010, Atmos. Chem. Phys., 12,
 37 8257-8270, 10.5194/acp-12-8257-2012, 2012.

38 Novelli, A., Hens, K., Tatum Ernest, C., Kubistin, D., Regelin, E., Elste, T., Plass-Dülmer,
 39 C., Martinez, M., Lelieveld, J., and Harder, H.: Characterisation of an inlet pre-injector laser-
 40 induced fluorescence instrument for the measurement of atmospheric hydroxyl radicals,
 41 Atmos. Meas. Tech., 7, 3413-3430, 10.5194/amt-7-3413-2014, 2014a.

42 Novelli, A., Vereecken, L., Lelieveld, J., and Harder, H.: Direct observation of OH formation
 43 from stabilised Criegee intermediates, Phys Chem Chem Phys, 16, 19941-19951,
 44 10.1039/c4cp02719a, 2014b.

1 Ouyang, B., McLeod, M. W., Jones, R. L., and Bloss, W. J.: NO₃ radical production from the
 2 reaction between the Criegee intermediate CH₂OO and NO₂, *Phys Chem Chem Phys*, 15,
 3 17070-17075, 10.1039/c3cp53024h, 2013.

4 Paulson, S. E., and Orlando, J. J.: The reactions of ozone with alkenes: An important source
 5 of HO_x in the boundary layer, *Geophys Res Lett*, 23, 3727-3730, 10.1029/96gl03477, 1996.

6 Paulson, S. E., Chung, M. Y., and Hasson, A. S.: OH Radical Formation from the Gas-Phase
 7 Reaction of Ozone with Terminal Alkenes and the Relationship between Structure and
 8 Mechanism, *The Journal of Physical Chemistry A*, 103, 8125-8138, 10.1021/jp991995e,
 9 1999.

10 Peeters, J., Boullart, W., Pultau, V., Vandenberg, S., and Vereecken, L.: Structure–Activity
 11 Relationship for the Addition of OH to (Poly)alkenes: Site-Specific and Total Rate
 12 Constants, *The Journal of Physical Chemistry A*, 111, 1618-1631, 10.1021/jp066973o, 2007.

13 Percival, C. J., Welz, O., Eskola, A. J., Savee, J. D., Osborn, D. L., Topping, D. O., Lowe, D.,
 14 Utembe, S. R., Bacak, A., McFiggans, G., Cooke, M. C., Xiao, P., Archibald, A. T., Jenkin,
 15 M. E., Derwent, R. G., Riipinen, I., Mok, D. W., Lee, E. P., Dyke, J. M., Taatjes, C. A., and
 16 Shallcross, D. E.: Regional and global impacts of Criegee intermediates on atmospheric
 17 sulphuric acid concentrations and first steps of aerosol formation, *Faraday Discuss*, 165, 45-
 18 73, 10.1039/c3fd00048f, 2013.

19 Petäjä, T., Mauldin, R. L., Kosciuch, E., McGrath, J., Nieminen, T., Paasonen, P., Boy, M.,
 20 Adamov, A., Kotiaho, T., and Kulmala, M.: Sulfuric acid and OH concentrations in a boreal
 21 forest site, *Atmospheric Chemistry and Physics*, 9, 7435-7448, 2009.

22 Pierce, J. R., Evans, M. J., Scott, C. E., D'Andrea, S. D., Farmer, D. K., Swietlicki, E., and
 23 Spracklen, D. V.: Weak global sensitivity of cloud condensation nuclei and the aerosol
 24 indirect effect to Criegee + SO₂ chemistry, *Atmos. Chem. Phys.*, 13, 3163-3176,
 25 10.5194/acp-13-3163-2013, 2013.

26 Plass-Dülmer, C., Michl, K., Ruf, R., and Berresheim, H.: C₂–C₈ Hydrocarbon measurement
 27 and quality control procedures at the Global Atmosphere Watch Observatory
 28 Hohenpeissenberg, *Journal of Chromatography A*, 953, 175-197,
 29 [http://dx.doi.org/10.1016/S0021-9673\(02\)00128-0](http://dx.doi.org/10.1016/S0021-9673(02)00128-0), 2002.

30 Rathman, W. C. D., Claxton, T. A., Rickard, A. R., and Marston, G.: A theoretical
 31 investigation of OH formation in the gas-phase ozonolysis of E-but-2-ene and Z-but-2-ene,
 32 *Phys Chem Chem Phys*, 1, 3981-3985, 10.1039/a903186c, 1999.

33 Ren, X., Harder, H., Martinez, M., Leshner, R. L., Oliger, A., Simpas, J. B., Brune, W. H.,
 34 Schwab, J. J., Demerjian, K. L., He, Y., Zhou, X., and Gao, H.: OH and HO₂ Chemistry in
 35 the urban atmosphere of New York City, *Atmos Environ*, 37, 3639-3651,
 36 [http://dx.doi.org/10.1016/S1352-2310\(03\)00459-X](http://dx.doi.org/10.1016/S1352-2310(03)00459-X), 2003.

37 Rickard, A. R., Johnson, D., McGill, C. D., and Marston, G.: OH Yields in the Gas-Phase
 38 Reactions of Ozone with Alkenes, *The Journal of Physical Chemistry A*, 103, 7656-7664,
 39 10.1021/jp9916992, 1999.

40 Ryzhkov, A. B., and Ariya, P. A.: A theoretical study of the reactions of carbonyl oxide with
 41 water in atmosphere: the role of water dimer, *Chemical Physics Letters*, 367, 423-429,
 42 [http://dx.doi.org/10.1016/S0009-2614\(02\)01685-8](http://dx.doi.org/10.1016/S0009-2614(02)01685-8), 2003.

1 Ryzhkov, A. B., and Ariya, P. A.: A theoretical study of the reactions of parent and
2 substituted Criegee intermediates with water and the water dimer, *Phys Chem Chem Phys*, 6,
3 5042-5050, 10.1039/b408414d, 2004.

4 Sarwar, G., Fahey, K., Kwok, R., Gilliam, R. C., Roselle, S. J., Mathur, R., Xue, J., Yu, J.,
5 and Carter, W. P. L.: Potential impacts of two SO₂ oxidation pathways on regional sulfate
6 concentrations: Aqueous-phase oxidation by NO₂ and gas-phase oxidation by Stabilized
7 Criegee Intermediates, *Atmos Environ*, 68, 186-197,
8 <http://dx.doi.org/10.1016/j.atmosenv.2012.11.036>, 2013.

9 Sarwar, G., Simon, H., Fahey, K., Mathur, R., Goliff, W. S., and Stockwell, W. R.: Impact of
10 sulfur dioxide oxidation by Stabilized Criegee Intermediate on sulfate, *Atmos Environ*, 85,
11 204-214, DOI 10.1016/j.atmosenv.2013.12.013, 2014.

12 Shallcross, D. E., Taatjes, C. A., and Percival, C. J.: Criegee intermediates in the indoor
13 environment: new insights, *Indoor Air*, n/a-n/a, 10.1111/ina.12102, 2014.

14 Sheps, L., Scully, A. M., and Au, K.: UV absorption probing of the conformer-dependent
15 reactivity of a Criegee intermediate CH₃CHOO, *Phys Chem Chem Phys*,
16 10.1039/c4cp04408h, 2014.

17 Shillings, A. J. L., Ball, S. M., Barber, M. J., Tennyson, J., and Jones, R. L.: An upper limit
18 for water dimer absorption in the 750 nm spectral region and a revised water line list, *Atmos.*
19 *Chem. Phys.*, 11, 4273-4287, 10.5194/acp-11-4273-2011, 2011.

20 Sinha, V., Williams, J., Crowley, J. N., and Lelieveld, J.: The Comparative Reactivity
21 Method – a new tool to measure total OH Reactivity in ambient air, *Atmos. Chem.*
22 *Phys.*, 8, 2213-2227, 10.5194/acp-8-2213-2008, 2008.

23 Sipilä, M., Jokinen, T., Berndt, T., Richters, S., Makkonen, R., Donahue, N. M., Mauldin Iii,
24 R. L., Kurtén, T., Paasonen, P., Sarnela, N., Ehn, M., Junninen, H., Rissanen, M. P.,
25 Thornton, J., Stratmann, F., Herrmann, H., Worsnop, D. R., Kulmala, M., Kerminen, V. M.,
26 and Petäjä, T.: Reactivity of stabilized Criegee intermediates (sCIs) from isoprene and
27 monoterpene ozonolysis toward SO₂ and organic acids, *Atmos. Chem. Phys.*, 14, 12143-
28 12153, 10.5194/acp-14-12143-2014, 2014.

29 Smith, M. C., Chang, C.-H., Chao, W., Lin, L.-C., Takahashi, K., Boering, K. A., and Lin, J.
30 J.-M.: Strong Negative Temperature Dependence of the Simplest Criegee Intermediate
31 CH₂OO Reaction with Water Dimer, *The Journal of Physical Chemistry Letters*, 2708-2713,
32 10.1021/acs.jpcllett.5b01109, 2015.

33 Smith, M. C., Chao, W., Takahashi, K., Boering, K. A., and Lin, J. J.-M.: Unimolecular
34 Decomposition Rate of the Criegee Intermediate (CH₃)₂COO Measured Directly with UV
35 Absorption Spectroscopy, *The Journal of Physical Chemistry A*, 10.1021/acs.jpca.5b12124,
36 2016.

37 Stone, D., Blitz, M., Daubney, L., Howes, N. U., and Seakins, P.: Kinetics of CH₂OO
38 reactions with SO₂, NO₂, NO, H₂O and CH₃CHO as a function of pressure, *Phys Chem Chem*
39 *Phys*, 16, 1139-1149, 10.1039/c3cp54391a, 2014.

40 Taatjes, C. A., Welz, O., Eskola, A. J., Savee, J. D., Scheer, A. M., Shallcross, D. E.,
41 Rotavera, B., Lee, E. P., Dyke, J. M., Mok, D. K., Osborn, D. L., and Percival, C. J.: Direct
42 measurements of conformer-dependent reactivity of the Criegee intermediate CH₃CHOO,
43 *Science*, 340, 177-180, 10.1126/science.1234689, 2013.

1 Taatjes, C. A., Shallcross, D. E., and Percival, C. J.: Research frontiers in the chemistry of
2 Criegee intermediates and tropospheric ozonolysis, *Phys Chem Chem Phys*, 16, 1704-1718,
3 10.1039/c3cp52842a, 2014.

4 Tan, Z., Fuchs, H., Lu, K., Bohn, B., Broch, S., Dong, H., Gomm, S., Haeseler, R., He, L.,
5 Hofzumahaus, A., Holland, F., Li, X., Liu, Y., Lu, S., Rohrer, F., Shao, M., Wang, B., Wang,
6 M., Wu, Y., Zeng, L., Zhang, Y., Wahner, A., and Zhang, Y.: Radical chemistry at a rural site
7 (Wangdu) in the North China Plain: Observation and model calculations of OH, HO₂ and
8 RO₂ radicals, *Atmos. Chem. Phys. Discuss.*, 2016, 1-48, 10.5194/acp-2016-614, 2016.

9 Tobias, H. J., and Ziemann, P. J.: Kinetics of the Gas-Phase Reactions of Alcohols,
10 Aldehydes, Carboxylic Acids, and Water with the C¹³ Stabilized Criegee Intermediate
11 Formed from Ozonolysis of 1-Tetradecene, *The Journal of Physical Chemistry A*, 105, 6129-
12 6135, 10.1021/jp004631r, 2001.

13 Vereecken, L., and Francisco, J. S.: Theoretical studies of atmospheric reaction mechanisms
14 in the troposphere, *Chemical Society Reviews*, 41, 6259-6293, 10.1039/c2cs35070j, 2012.

15 Vereecken, L., Harder, H., and Novelli, A.: The reaction of Criegee intermediates with NO,
16 RO₂, and SO₂, and their fate in the atmosphere, *Phys Chem Chem Phys*, 14, 14682-14695,
17 10.1039/c2cp42300f, 2012.

18 Vereecken, L., Harder, H., and Novelli, A.: The reactions of Criegee intermediates with
19 alkenes, ozone, and carbonyl oxides, *Phys Chem Chem Phys*, 16, 4039-4049,
20 10.1039/c3cp54514h, 2014.

21 Vereecken, L., Glowacki, D. R., and Pilling, M. J.: Theoretical Chemical Kinetics in
22 Tropospheric Chemistry: Methodologies and Applications, *Chemical Reviews*,
23 10.1021/cr500488p, 2015.

24 Wayne, R. P.: *Chemistry of Atmosphere*, Oxford University Press: Oxford, 2000.

25 Welz, O., Savee, J. D., Osborn, D. L., Vasu, S. S., Percival, C. J., Shallcross, D. E., and
26 Taatjes, C. A.: Direct Kinetic Measurements of Criegee Intermediate (CH₂OO) Formed by
27 Reaction of CH₂I with O₂, *Science*, 335, 204-207, 10.1126/science.1213229, 2012.

28 White, J. U.: Long optical paths of large aperture, *J. Opt. Soc. Am.*, 32, 285-288,
29 10.1364/josa.32.000285, 1942.

30 Williams, J., Crowley, J., Fischer, H., Harder, H., Martinez, M., Petäjä, T., Rinne, J., Bäck, J.,
31 Boy, M., Dal Maso, M., Hakala, J., Kajos, M., Keronen, P., Rantala, P., Aalto, J., Aaltonen,
32 H., Paatero, J., Vesala, T., Hakola, H., Levula, J., Pohja, T., Herrmann, F., Auld, J.,
33 Mesarchaki, E., Song, W., Yassaa, N., Nölscher, A., Johnson, A. M., Custer, T., Sinha, V.,
34 Thieser, J., Pouvesle, N., Taraborrelli, D., Tang, M. J., Bozem, H., Hosaynali-Beygi, Z.,
35 Axinte, R., Oswald, R., Novelli, A., Kubistin, D., Hens, K., Javed, U., Trawny, K.,
36 Breitenberger, C., Hidalgo, P. J., Ebben, C. J., Geiger, F. M., Corrigan, A. L., Russell, L. M.,
37 Ouwersloot, H. G., Vilà-Guerau de Arellano, J., Ganzeveld, L., Vogel, A., Beck, M., Bayerle,
38 A., Kampf, C. J., Bertelmann, M., Köllner, F., Hoffmann, T., Valverde, J., González, D.,
39 Riekkola, M. L., Kulmala, M., and Lelieveld, J.: The summertime Boreal forest field
40 measurement intensive (HUMPPA-COPEC-2010): an overview of meteorological and
41 chemical influences, *Atmos. Chem. Phys.*, 11, 10599-10618, 10.5194/acp-11-10599-2011,
42 2011.

1 Woodward-Massey, R., Cryer, D. R., Whalley, L. K., Ingham, T., Seakins, P. W., Heard, D.
2 E., and Stimpson, L. M.: Implementation of a chemical background method (OH-CHEM) for
3 measurements of OH using the Leeds FAGE instrument: Characterisation and observations
4 from a coastal location. , Abstract A41A-0002 presented at 2015 Fall Meeting, AGU, San
5 Francisco, Calif., 14-18 Dec, 2015.

6 Yassaa, N., Song, W., Lelieveld, J., Vanhatalo, A., Back, J., and Williams, J.: Diel cycles of
7 isoprenoids in the emissions of Norway spruce, four Scots pine chemotypes, and in Boreal
8 forest ambient air during HUMPPA-COPEC-2010, Atmospheric Chemistry and Physics, 12,
9 7215-7229, 10.5194/acp-12-7215-2012, 2012.

10 York, D., Evensen, N. M., Martínez, M. L., and De Basabe Delgado, J.: Unified equations for
11 the slope, intercept, and standard errors of the best straight line, American Journal of Physics,
12 72, 367-375, doi:<http://dx.doi.org/10.1119/1.1632486>, 2004.

13 Zhang, D., and Zhang, R.: Mechanism of OH Formation from Ozonolysis of Isoprene: A
14 Quantum-Chemical Study, J Am Chem Soc, 124, 2692-2703, 10.1021/ja011518l, 2002.

15 Zhu, C., Kumar, M., Zhong, J., Li, L., Francisco, J. S., and Zeng, X. C.: New Mechanistic
16 Pathways for Criegee–Water Chemistry at the Air/Water Interface, J Am Chem Soc,
17 10.1021/jacs.6b04338, 2016.

18
19
20

1 Table 1. Average concentration (molecule cm⁻³), with 1σ variability, of trace gases relevant for this
2 study.

Compound	HUMPPA-COPEC 2010	HOPE 2012
SO ₂ ^a	(1.4 ± 1.7) x 10 ¹⁰	(2.2 ± 2.3) x 10 ⁹
H ₂ SO ₄ ^a	(2 ± 2) x 10 ⁶	(8.5 ± 8.5) x 10 ⁵
OH ^a	(7 ± 8) x 10 ⁵	(1.6 ± 1.6) x 10 ⁶
O ₃ ^a	(1.1 ± 0.2) x 10 ¹²	(1.1 ± 0.3) x 10 ¹²
Σ[VOC] ^{a,b}	(7.3 ± 7.1) x 10 ⁹	(9.8 ± 9.0) x 10 ⁹
OH Reactivity ^c	9.0 ± 7.6	3.5 ± 3.0
Condensation sink (CS) ^c	(10 ± 4.0) x 10 ⁻³	(7 ± 3) x 10 ⁻³

3 a, Units: molecules cm⁻³.

4 b, HUMPPA COPEC 2010: isoprene, (-)/(+) α-pinene, (-)/(+) β-pinene, 3-carene, and
5 myrcene.

6 HOPE 2012: isoprene, α-pinene, β-pinene, 3-carene, myrcene, limonene, 2-
7 methylpropene, but-1-ene, sabinene, γ-terpinene, propene, cis-2-butene and ethene.

8 c, Units: s⁻¹.

9 1 ppbv = 2.46 x 10¹⁰ molecules cm⁻³ at 295K and 1013 hPa.

1 Table 2. SCI estimates for the HUMPPA-COPEC 2010 and HOPE 2012 campaigns. Average
2 concentration (molecule cm⁻³), with 1σ variability.

Approach	HUMPPA-COPEC 2010	HOPE 2012
Missing H ₂ SO ₄	(2.3 ± 2) x 10 ⁴ ^a	(2.0 ± 3) x 10 ⁴ ^a
	(1.6 ± 2) x 10 ⁶ ^b	(1 ± 3) x 10 ⁶ ^b
Measured unsaturated VOC	(5 ± 4) x 10 ³	(7 ± 6) x 10 ³
Unexplained OH reactivity	(1 ± 1) x 10 ⁵	(2 ± 1.5) x 10 ⁴
Unexplained OH production	(2 ± 2) x 10 ⁴ ^c	n. a.
	(4 ± 4) x 10 ⁵ ^d	n. a.

3 a, $k_{\text{SCI}+\text{SO}_2} = 3.3 \times 10^{-11} \text{ cm}^3 \text{ molecule}^{-1} \text{ s}^{-1}$

4 b, $k_{\text{SCI}+\text{SO}_2} = 5 \times 10^{-13} \text{ cm}^3 \text{ molecule}^{-1} \text{ s}^{-1}$

5 c, $P_{\text{OH}}^{\text{unexplained}} = 1 \times 10^6 \text{ molecule cm}^{-3} \text{ s}^{-1}$

6 d, $P_{\text{OH}}^{\text{unexplained}} = 2 \times 10^7 \text{ molecule cm}^{-3} \text{ s}^{-1}$

7 1 ppbv = $2.46 \times 10^{10} \text{ molecules cm}^{-3}$ at 295K and 1013 hPa.

8

9

10

11

12

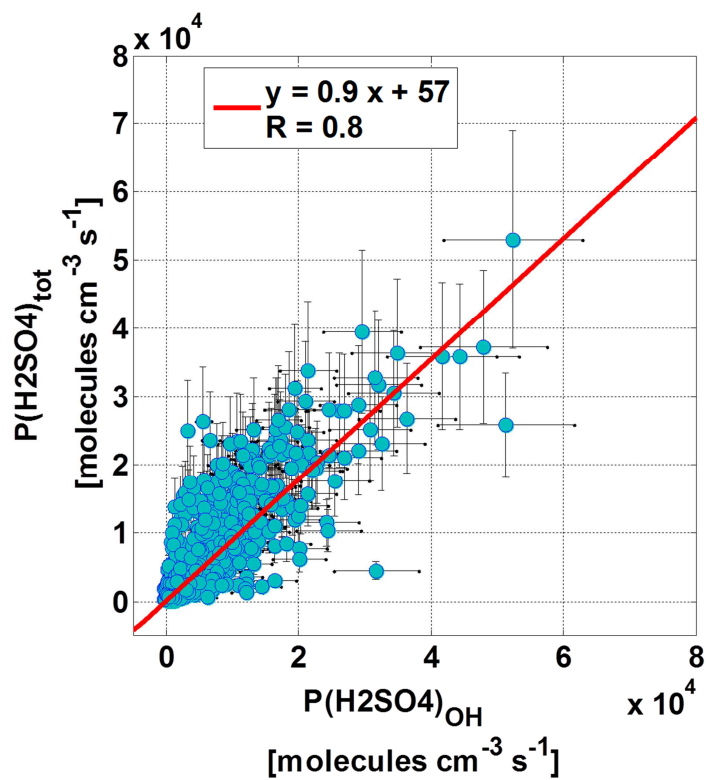
13

14

15

16

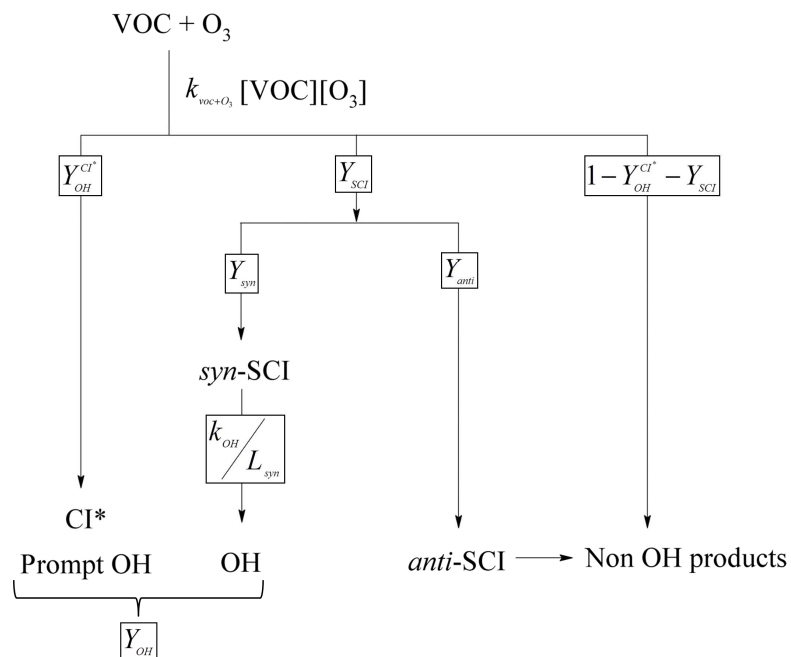
17



1

2 Figure 1. Total production rate of H_2SO_4 ($P(\text{H}_2\text{SO}_4)_{\text{tot}}$) as a function of the production rate of
 3 H_2SO_4 from the reaction between OH and SO_2 during the HOPE 2012 campaign. The linear
 4 regression, following the method of York et al. (2004), yields a slope of 0.9 ± 0.02 and a
 5 intercept of 57 ± 7 .

6



1

2 Figure 2. Schematic representation of the formation of OH from the ozonolysis of unsaturated

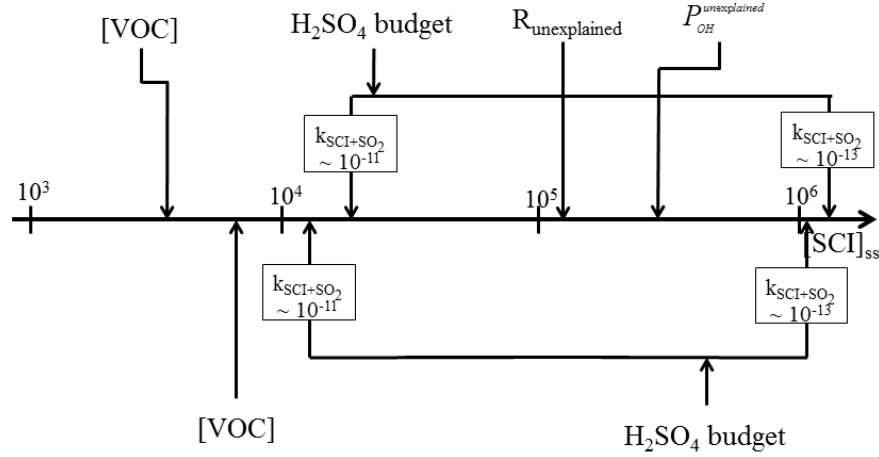
3 VOC.

4

5

6

Boreal Forest (HUMPPA-COPEC 2010)



(Rural Europe)HOPE 2012

Figure 3. Schematic overview of the estimated steady state concentration of SCI ($[SCI]_{ss}$, molecules cm^{-3}) observed during the HUMPPA-COPEC 2010 and HOPE 2012 campaigns. For both campaigns the SCI estimate is based on the unsaturated VOC concentration measured, $[VOC]$, and the H_2SO_4 budget using different $\text{SCI}+\text{SO}_2$ rate coefficients ($k_{\text{SCI}+\text{SO}_2}$ in $\text{cm}^3 \text{ molecule}^{-1} \text{ s}^{-1}$). In addition, during the HUMPPA-COPEC campaign SCI can be calculated from the unexplained OH reactivity, $R_{\text{unexplained}}$, and unexplained OH production, $P_{\text{unexplained}}^{\text{OH}}$. See main text for more details (Section 3).

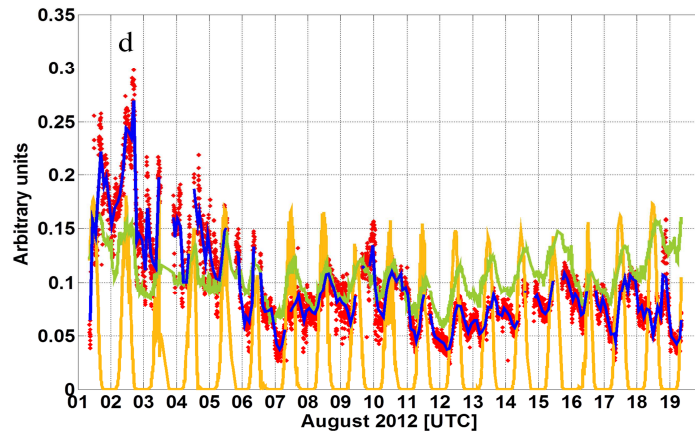
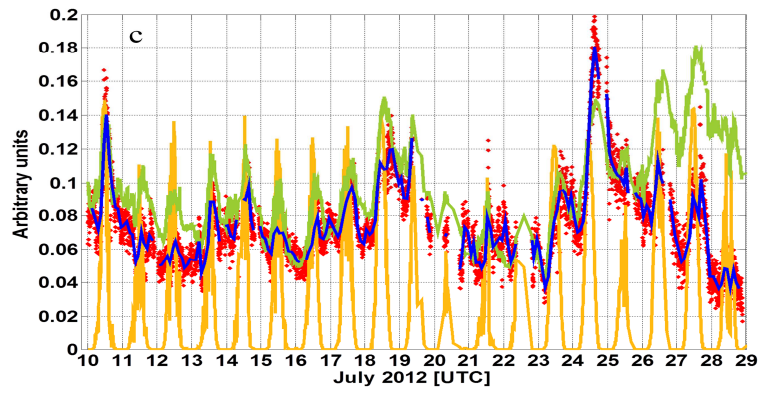
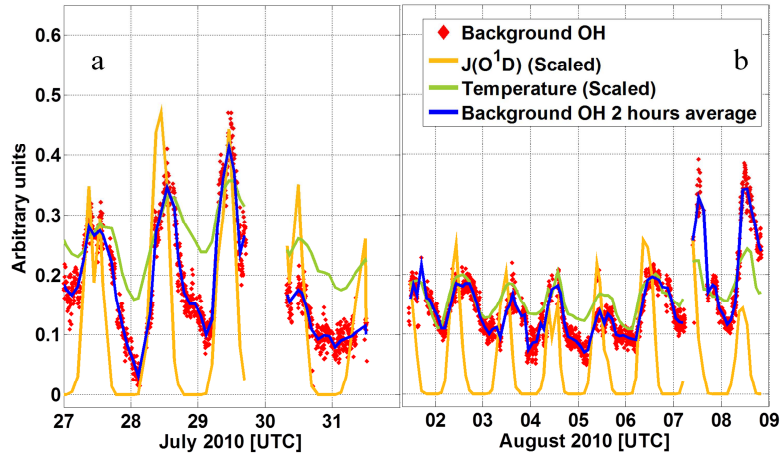
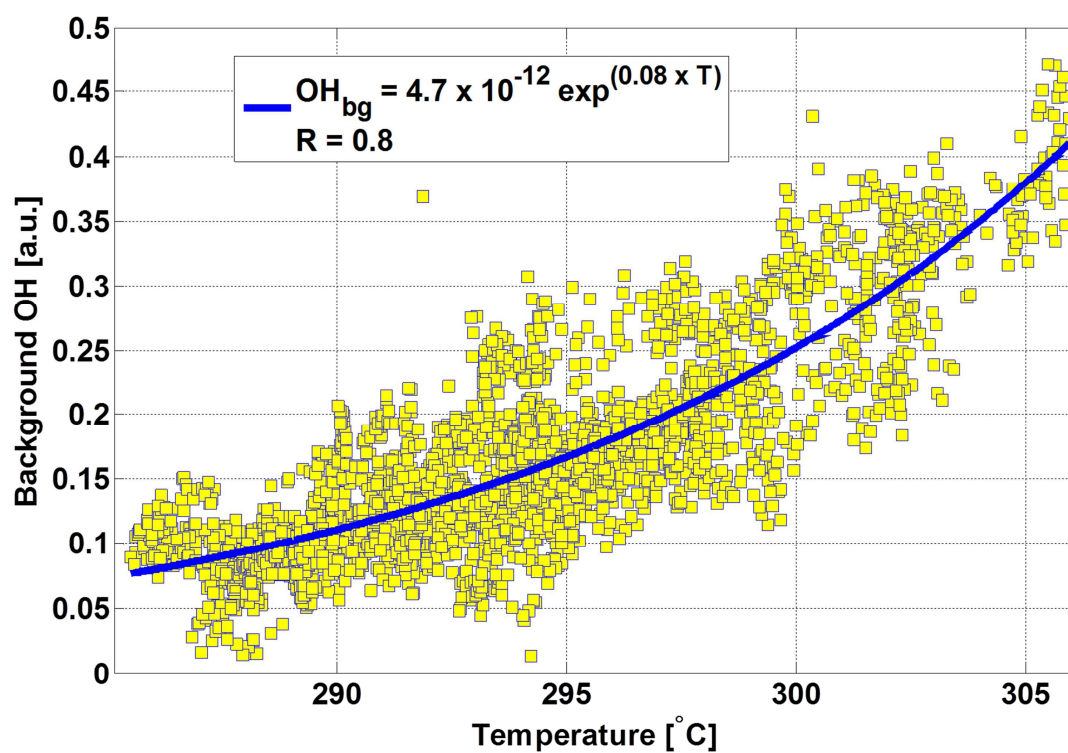


Figure 4. Background OH (red diamonds) measured during the HUMPPA-COPEC 2010 (a, ground and b, tower) and the HOPE 2012 (c, July and d, August) campaigns together with scaled $J(O^1D)$, multiplied by 4×10^4 and 4×10^3 for HUMPPA-COPEC 2010 and HOPE 2012, respectively (orange), and scaled temperature divided by 90 and 160 K for HUMPPA-COPEC 2010 and HOPE 2012, respectively (green).



1

2 Figure 5. Background OH as a function of the temperature during the HUMPPA-COPEC
 3 2010 campaign.

4

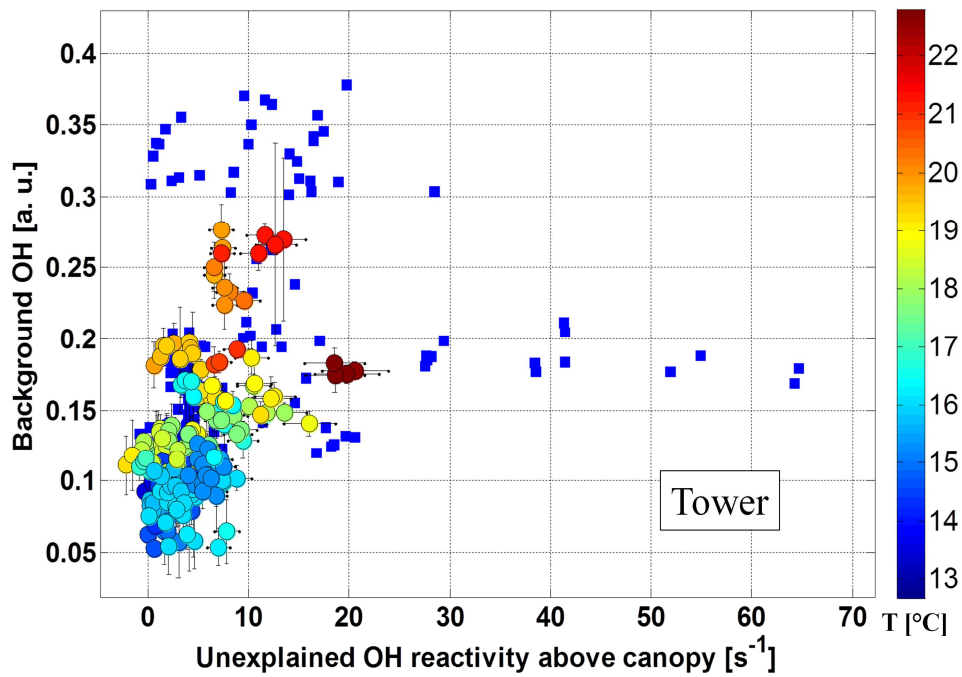
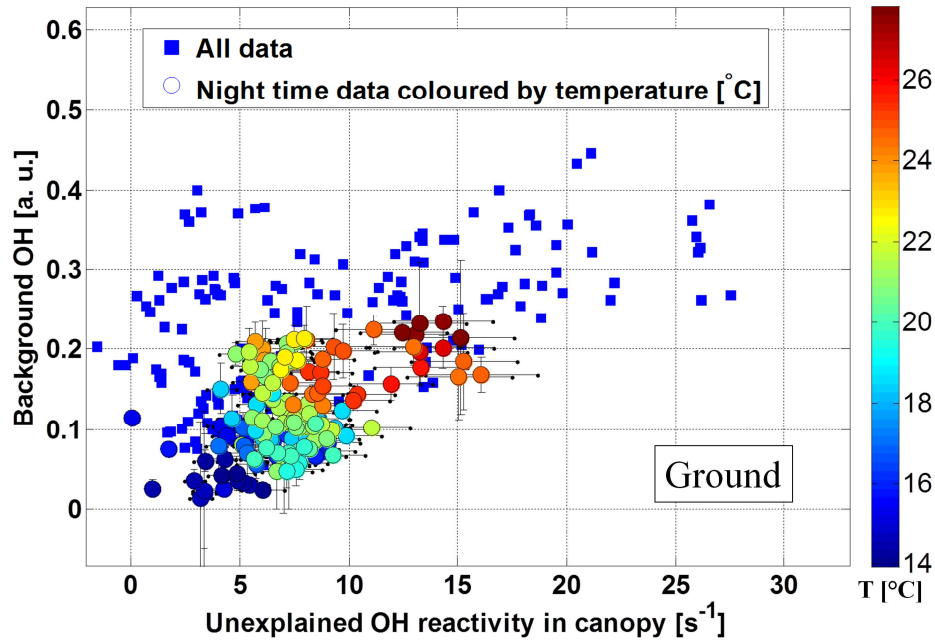
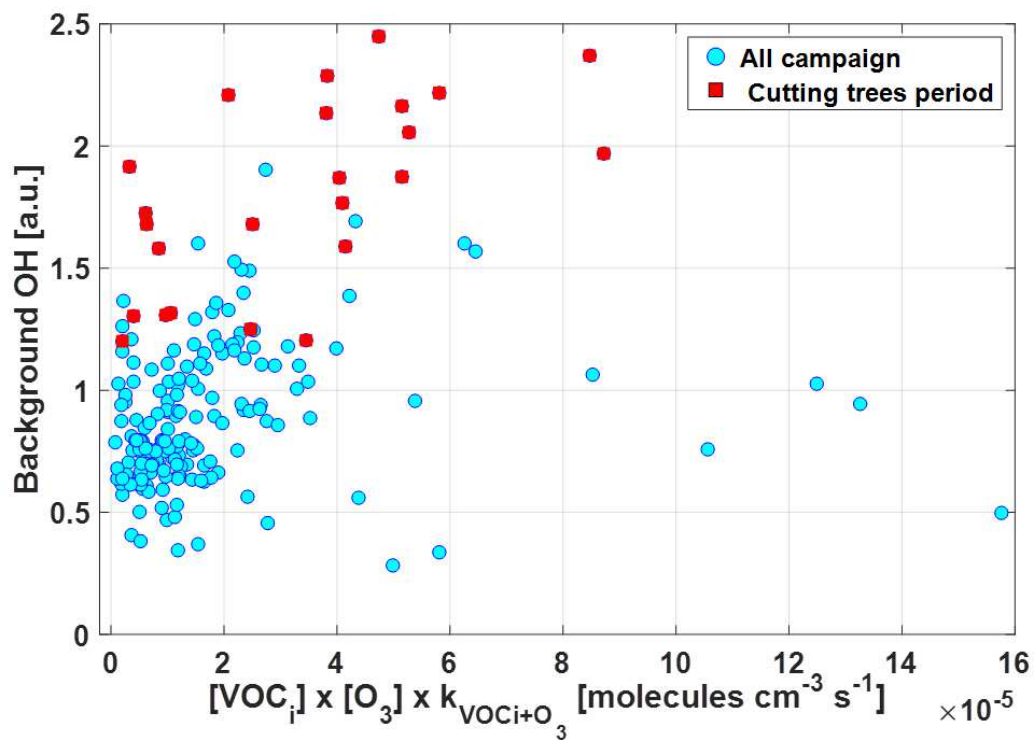


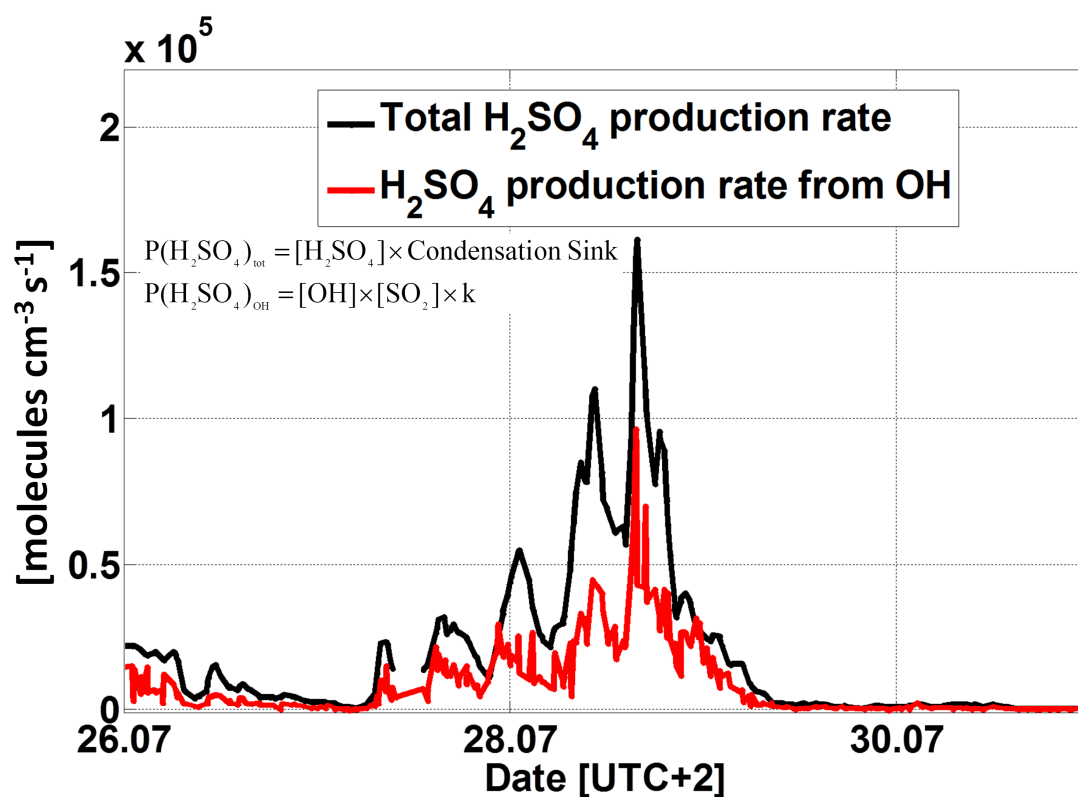
Figure 6. Background OH as a function of unexplained OH reactivity for ground and tower period measurements during the HUMPPA-COPEC 2010 campaign. Squares represent the daytime data, bullets represent night time data and are coloured accordingly to temperature (right legend).



1

2 Figure 7. Background OH as a function of the sum of the product of the measured
 3 unsaturated VOC-ozone turn-over (Table SI-1), during the HOPE 2012 campaign. The blue
 4 points refer to the entire field campaign excluding tree cutting, which occurred between 1st
 5 and 3rd of August 2012, described by the red squares.

6



1

2 Figure 8. Comparison of the total H_2SO_4 production rate (black line), calculated from the
 3 measured H_2SO_4 , and the production rate of H_2SO_4 (red line) involving only the oxidation
 4 process of SO_2 by OH for the ground measurements during the HUMPPA-COPEC 2010
 5 campaign.

6

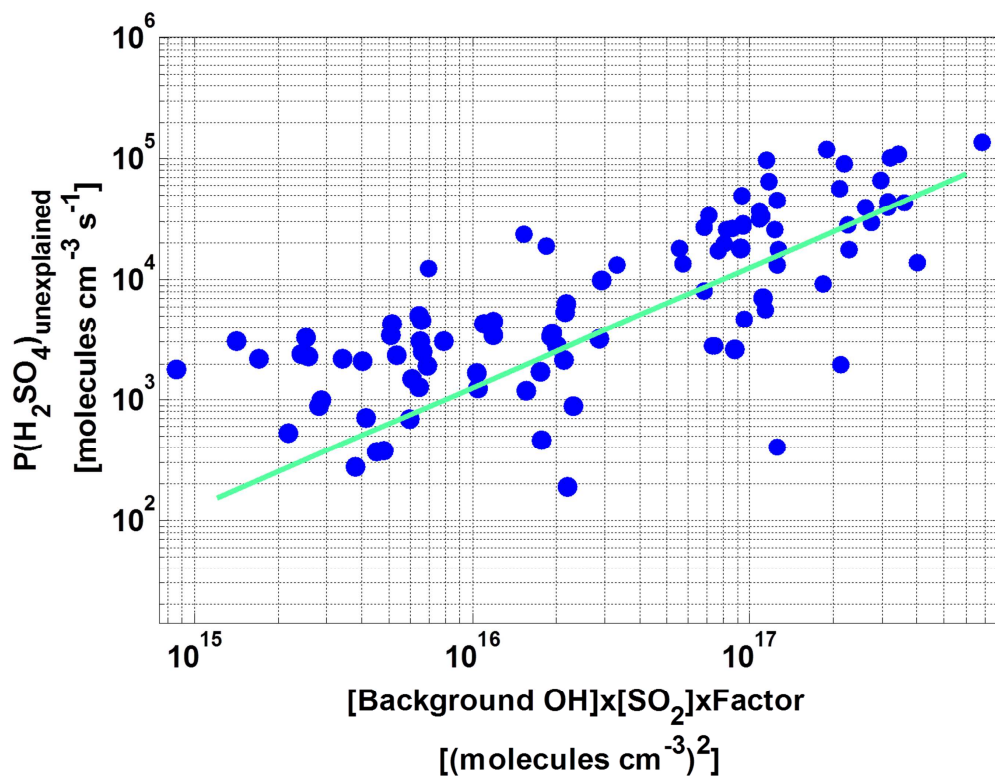
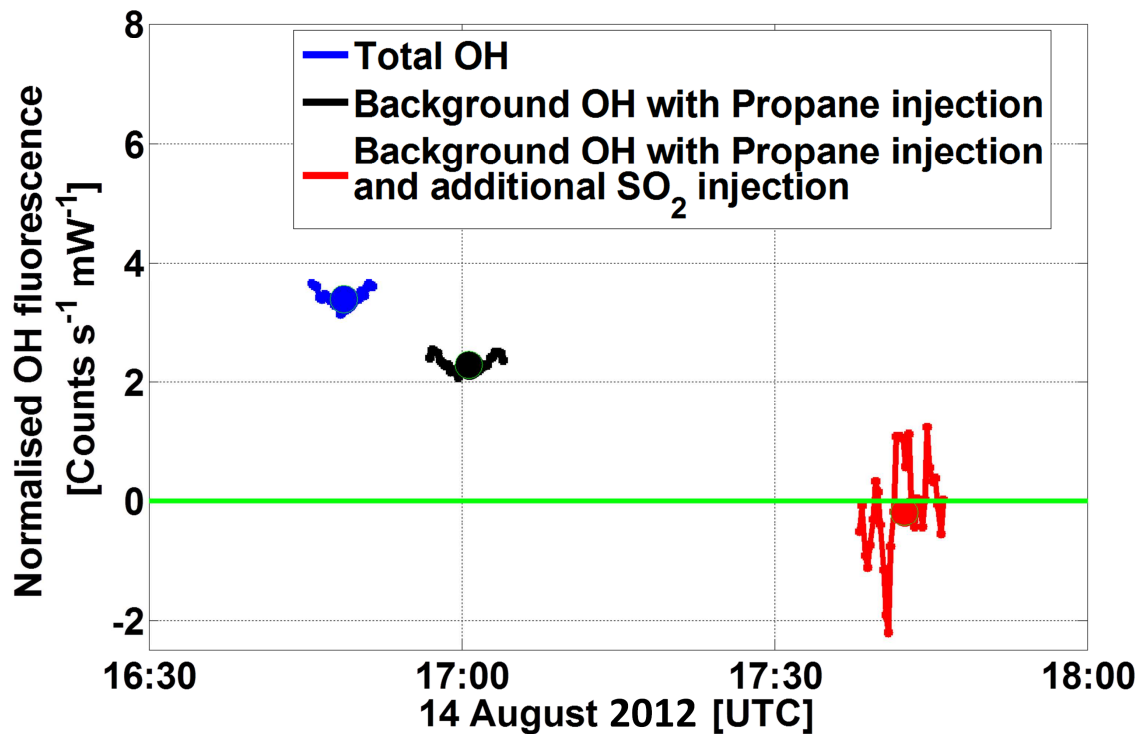


Figure 9. The production rate of H_2SO_4 unaccounted for by the oxidation of SO_2 by OH as a function of the OH_{bg} multiplied by SO_2 concentration during the ground measurements of the HUMPPA-COPEC 2010 campaign. OH_{bg} is expressed in molecules cm^{-3} equivalents of OH.



1
2 Figure 10. SO₂ injection test within IPI during the HOPE 2012 campaign. The blue data
3 points represent the total OH measured when no injection is performed. The black data points
4 represent the background OH measured while injecting propane (2.5×10^{15} molecules cm⁻³)
5 scavenging > 90 % of ambient OH. The red signal is the background OH observed when SO₂
6 (1×10^{13} molecules cm⁻³) is injected in addition to propane.

7